Computer Networks 93 (2015) 225–242

Contents lists available at ScienceDirect

Computer Networks

journal homepage: www.elsevier.com/locate/comnet

Multiple many-to-many multicast routing scheme in green multi-granularity transport networks

Xingwei Wang[a], Dapeng Qu[b,*], Min Huang[c], Keqin Li[d], Sajal K. Das[e], Jinhong Zhang[c], Ruiyun Yu[a]

[a] College of Software, Northeastern University, Shenyang 110819, China
[b] College of Information, Liaoning University, Shenyang 110036, China
[c] College of Information Science and Engineering, Northeastern University, Shenyang 110819, China
[d] Department of Computer Science, State University of New York, New Paltz, New York 12561, USA
[e] Department of Computer Science, Missouri University of Science and Technology, Rolla, Missouri 65409, USA

ARTICLE INFO

Article history:
Received 2 February 2015
Revised 30 July 2015
Accepted 21 October 2015
Available online 2 November 2015

Keywords:
Green multi-granularity transport networks
Multiple many-to-many multicast
Routing
Power efficiency
QoS
Resource utilization

ABSTRACT

Due to the ubiquitous use of the Internet and huge proliferation of network devices, the energy consumed by today's networks has increased significantly, implying the need for designing and operating green networks. In this paper, we propose a power-efficient Quality of Service (QoS) routing scheme for multiple many-to-many multicast requests with given static traffic demands in green multi-granularity transport networks, which comprehensively considers both the IP and the optical layers. A chosen probability model is devised to describe the probability of a link being selected when routing, and a heuristic routing algorithm is proposed to construct multiple many-to-many multicast trees in order to decrease power consumption, enhance QoS evaluation and improve resource utilization evaluation under QoS and capacity constraints. Results from simulation experiments demonstrate that our proposed scheme is more power-efficient with higher QoS evaluation and better resource utilization compared with others.

1. Introduction

Due to the rapid development of Information and Communication Technology (ICT) and a wide variety of networked applications, today's Internet consumes a significant amount of energy. In the US alone, Internet used 9.4% of the produced electricity and this Internet electricity cost keeps increasing every year [1]. Therefore, green or energy saving network is emerging as an active area of research on networking and communication [2]. Moreover, most of the current (wired) network resources are considered redundant in order to guarantee reliability; the maximum utilization ratio of the backbone network is often less than 30% even in the working state [3]. This makes it feasible to realize green networks.

There are a lot of researches and developments already existed in green networks based on the IP layer, for example, manufacturing energy-efficient routers [4], making networking devices sleep periodically [5], and so on. However, it is not enough to develop green networks just based on the IP layer. In fact, in the current Internet, the network traffic (in the IP layer) is transmitted on the fiber backbone (optical layer) in order that the flexibility of the IP layer and the huge bandwidth of the optical layer can be exploited [6]. Therefore, with the worldwide fiber deployment and advanced Wavelength Division Multiplexing (WDM) technologies, multi-granularity transport networks have been introduced [7]. By multiplexing many IP layer services into one wavelength and in turn multiplexing dozens of wavelengths into one waveband, and so on, bandwidth utilization is

* Corresponding author: Tel: +86 2462202242
E-mail address: dapengqu@lnu.edu.cn, dapengqu@126.com (D. Qu).

http://dx.doi.org/10.1016/j.comnet.2015.10.015

significantly improved. There is no doubt that multi-granularity transport networks should be green and energy saving.

The energy saving mechanism can be divided into node-wise type and network-wise type. The former achieves energy saving by adjusting the component's working status in the node and link and trying to make its energy consumption be proportional to its transferred traffic. The latter achieves energy saving by improving the existing or re-designing new network architectures, protocols or algorithms. As a network-wise energy saving mechanism, the green routing issue has attracted wide attention. However, most of the current researches have so far focused on energy-constrained networks, such as mobile/wireless networks and satellite-based networks [8–10]. Even for the backbone networks, existing energy saving routing mechanisms are often focused either on the IP layer or the optical layer [11–17]. However, in multi-granularity transport networks, energy saving should be considered not only in the IP layer but also in the optical layer, so that energy efficiency could be further increased compared with the case when only one single layer is considered. Therefore, a power-efficient routing scheme should be developed in green multi-granularity transport networks, taking both IP and optical layer energy saving into account in an integrated way.

With various kinds of new networked applications, especially multimedia based ones, emerged, and with user demands diversified, Quality of Service (QoS) support becomes critical to networks. For example, video conference often has tight requirement on the bandwidth, delay and delay jitter and relatively loose requirement on loss, while bulk data transfer often has tight requirement on the bandwidth and transfer reliability and relatively loose requirement on delay and delay jitter. Therefore, the QoS requirements of the applications, especially their requirements on bandwidth, delay, delay jitter and error rate, should be considered by the routing scheme, so that their users can get high Quality of Experience (QoE) [18].

Meanwhile, making energy consumption adaptive to the transferred traffic is an effective way to save energy in green multi-granularity transport networks. Traffic demands should be routed with guidance to promote traffic to traverse the already-in-use network components (such as routers, switches and links) as many as possible, and thus network resource utilization can be improved significantly. In fact, with traffic aggregated to certain network components, the unused components can be put into low-power sleep mode or even switched off [19], and then substantial energy can be saved compared with the situation under which network devices are active no matter whether there are traffics transferred by them. Therefore, to make network energy consumption be traffic adaptive, resource utilization evaluation should be used as an energy-saving indicator to guide the power-efficient routing.

When designing a power-efficient routing scheme in green multi-granularity transport networks, we also need to consider the application's communication type. According to the amount of participants, it can be classified into unicast, multicast and broadcast; and multicast can be further divided into one-to-many and many-to-many. Existing researches pay more attention to unicast, one-to-many multicast and broadcast. However, certain kinds of applications need many-to-many multicast support and their demands are often known in advance, for example, video conference, telemedicine consultation and cyber games, etc. As an example, consider a multinational corporation which holds a video conference among all managers from different regions for production plan every Monday at 9:00 am. For such kinds of given static traffic demands, the routes could be computed and the required resources could be reserved in advance with the QoS requirements satisfied.

In this paper, we propose a Power-efficient QoS Routing Scheme (*PQRS*) in green multi-granularity transport networks to support Multiple Many-to-many Multicast Requests (M^3R) with given static traffic demands, in particular, their QoS requirements are known in advance and they will be started up at the same time. The contributions of our work are summarized as follows:

(1) The *PQRS* not only takes IP and optical layers into account integratedly, but also optimizes power consumption, QoS evaluation and resource utilization evaluation simultaneously under QoS and capacity constraints. To our best knowledge, it is the first one which deals with all the above factors comprehensively.
(2) The quantitative models of power consumption, QoS evaluation and resource utilization evaluation for nodes, links, branches, and trees are devised respectively, which provide the basis for the optimized tree construction when routing is done.
(3) A Chosen Probability Model (*CPM*) is presented to describe the property of the link in the network comprehensively, and its value denotes the probability of a link being chosen enroute along the tree. With *CPM*, a link with good performance on power consumption, QoS evaluation and resource utilization evaluation is preferred when routing.
(4) A heuristic Routing algorithm based on the *CPM* (*RCPM*) is proposed to construct tree or trees for M^3R. In particular, a multiplexing phase is devised to promote traffics to traverse along the same routes and to use the same active components as many as possible, and thus help avoid newly activating components and reduce power consumption further.

The rest of this paper is organized as follows. The related work is reviewed in Section 2. The problem formulation is introduced in Section 3. The algorithm description is given in Section 4. Simulation study is presented in Section 5. Conclusion is drawn in Section 6.

2. Related work

For the node-wise energy saving mechanisms, some new energy saving routers have been proposed, such as green router [20], dynamic energy router [21], and green reconfigurable router [22], and so on. These newly designed routers achieve power efficiency mainly through adaptive rate processing or power-aware packet forwarding, etc. For example, in [22], the router is reconfigurable in its settings (e.g., routing path, clock frequency, and supply voltage) based on its awareness of traffic rate fluctuations to reduce both average and peak power consumption during network operation.

For the network-wise energy saving mechanisms, a large amount of existent researches focus on mobile/wireless networks and satellite-based networks, such as [8–10], which are beyond the scope of this paper. For the backbone networks, there are some energy saving routing mechanisms. In [11], an energy saving routing scheme is proposed, which allows the incoming flows to be autonomously aggregated on some heavy-loaded links and switches off other light-loaded links. In [12], the current link-state routing protocols, for example, Open Shortest Path First (OSPF), are modified to achieve network-wise energy saving. Certain links are powered off during low traffic periods and the new paths are computed again on the modified network topology. In [13], three hop-by-hop green routing algorithms are presented, which are loop-free, maximize energy conservation, and jointly consider green and QoS requirements respectively. In [14], a service level agreement based hybrid green routing approach is proposed, which takes CO_2 emission rate, path length and path availability as the route selection criteria. In [15], a total power consumption model of an optical WDM network is proposed in terms of power consumed by individual lightpath, and an Integer Linear Programming (ILP) formulation for the solved problem is developed. In [16], the auxiliary graph based heuristics and energy-awareness are introduced into the green optical networks so that the currently active components are used as many as possible and thus substantial energy is saved in network operation. In [17], five energy aware routing approaches are proposed to simultaneously minimize energy consumption in WDM networks and the number of transitions from sleep to active mode while considering blocking rate. However, the above researches on energy saving routing focus only on one single layer. There are also some routing schemes which take both IP and optical layers into account in an integrated way and thus the energy efficiency could be further increased. In [23], a cross-layer optimization and design approach is proposed to improve the energy efficiency in IP over WDM backbone networks by controlling the maximum hop count and the maximum link utilization. In [24], the joint traffic scheduling and routing for delay bounded packet transmission across IP layer and WDM transport layer is proposed to improve energy and bandwidth efficiency. In [25], the mixed ILP based optimization models and the auxiliary matrix based network design heuristics are proposed for IP over WDM network to minimize the overall expenditure due to cost and energy consumption. In [26], a power-efficient integrated routing model in IP over WDM networks is proposed to manage resources at the IP layer and the optical layer together, thereby leading to higher flexibility and better resource utilization. Compared with the above researches, our proposed scheme not only takes energy saving across IP layer and optical layer into account in an integrated way, but also considers QoS (in terms of bandwidth, delay, delay jitter and error rate) evaluation and resource utilization evaluation comprehensively.

Most of the existing energy saving routing schemes in backbone networks do not consider the QoS requirements of networked applications [27], for example, QoS requirements are not considered in [11, 12, 14–16, 25]. Although the QoS requirements are investigated in [13, 17, 23, 24, 26], however, only the path stretch is considered in [13], only the blocking probability is considered in [17, 26], only the hop count is considered in [24], and the packet loss and delay are considered in [23]. On the other hand, most of the existing QoS routing schemes do not deal with energy saving [28]. However, in [29], a routing mechanism in multi-granularity transport networks is proposed with energy saving and QoS support considered simultaneously. Based on the devised novel node structure and link structure, the layered auxiliary graph (LAG) is constructed to support the integrated routing and grooming across the IP layer and the optical layer. A biogeography based intelligent method is used to provide the global optimization of network power consumption and user QoS satisfaction degree. In fact, its proposed power-efficient QoS routing mechanism is our previous work for this paper. The reader can refer to [29] for details. Moreover, to the best of our knowledge, the existent researches do not take resource utilization into account to guide traffic routing with power efficiency improved further, which is done in this paper.

In addition, existing researches on routing pay much more attention to unicast [29–30] and one-to-many multicast [31–36]. For example, the proposed routing scheme in [29] is oriented to the unicast scenario in multi-granularity transport networks. In [30], a joint admission control and unicast routing scheme is proposed to provide the energy saving online routing of flows with additive constraints, aiming at maximizing the number of admitted flow requests while minimizing the number of nodes and links that need to stay active. In [31], the greedy randomized adaptive search procedure is combined with the bounded shortest multicast algorithm to solve the so-called constrained minimum Steiner tree problem inherent in QoS multicast routing. In [32], the problem of multicast routing and wavelength assignment with delay constraint is investigated. An ILP model is formulated and used for the small-scale networks, while an efficient heuristic is used to produce the approximate solution for the large-scale networks in polynomial time. In [33], an ILP formulation is proposed for optimal assignments of hop constrained light-trees for multicast connections to maximize network throughput and improve resource utilization. In [34], node architecture and path computation element architecture are proposed to support and control optical multicast respectively. However, the above researches do not deal with the many-to-many multicast scenario. Although there are some researches which focus on multiple multicast requests, they also mainly deal with the one-to-many multicast scenario. In [35], a unified approach is proposed to construct multiple one-to-many multicast trees and find a max-min fair rate allocation among them to satisfy the link-capacity constraints. In [36], a heuristic procedure is employed to generate a tree for each one-to-many multicast request in isolation, and apply genetic algorithm to find the appropriate combination of these trees to meet the bandwidth requirements of the multiple multicast requests simultaneously. To the best of our knowledge, this paper is the first work on the power-efficient QoS routing scheme for multiple many-to-many multicast requests in green multi-granularity transport networks.

3. Problem formulation

In this section, we describe the models proposed for green multi-granularity transport networks and the multiple many-to-many multicast requests dealt with in this paper. Then, we formulate the problem mathematically which is solved in Section 4. In particular, we introduce the notations and terminologies defined in this paper.

3.1. Network model

A green multi-granularity transport network can be modeled as a graph $G = (V, E)$, where $V = \{v_i | 1 \le i \le N\}$ is the set of nodes, $E = \{e_{i,j} | v_i, v_j \in V,\ 1 \le i, j \le N,\ i \ne j\}$ is the set of links, and N is the total number of nodes in G, $N = |V|$.

Based on [29], we devise the node structure and the link structure with multicast extension for green multi-granularity transport networks shown in Fig. 1(a) and (b) respectively. A node consists of an IP layer module with Multicast Capable (MC) switching matrix, a Multi-Granularity Multicast Capable Optical Cross-Connect (MG-MC-OXC), a master engine with routing and switching controller and routing table, and optical transceivers (transmitters or receivers). Among them, the MG-MC-OXC consists of MC Wavelength Cross-Connect (MC-WXC), MC waveBand Cross-Connect (MC-BXC) and MC Fiber Cross-Connect (MC-FXC) with wavelength, waveband, and fiber as switching granularity respectively. These devices have power awareness and management functions. The proposed node structure considers power saving at the IP layer as well as the optical layer in an integrated way. A fiber link is deployed with an optical pre-amplifier, some optical in-line amplifiers, some optical regenerators, and an optical post-amplifier. The reader can refer to [29] for details. Compared with the node structure presented in [29], in order to support multicast, multi-granularity optical cross-connect and IP layer switching matrix are multicast capable. In particular, we assume that optical splitters are deployed in WXC, BXC and FBC with Splitter-and-Delivery (SaD) type of switching enabled [37, 38]. Because optical splitters are passive components and operate all-optically, we can consider that they bring no power consumption, no delay, no delay jitter and no error.

A $v_i \in V$ is associated with a quadruple (pc, dl, jt, er), and pc, dl, jt, and er represent power consumption, delay, delay jitter and error rate of v_i respectively. An $e_{i,j} \in E$ is associated with a nine-tuple (pc, bw, dl, jt, er, bwu, wlo, wbo, fbo), and pc, bw, dl, jt, er, bwu, wlo, wbo, and fbo represent power consumption, available bandwidth, delay, delay jitter, error rate, bandwidth utilization, namely the already-in-use bandwidth, wavelength occupancy, namely the number of the already-in-use wavelengths, waveband occupancy, namely the number of the already-in-use wavebands, and fiber occupancy, namely the number of the already-in-use fibers of $e_{i,j}$ respectively. In summary, pc belongs to power consumption parameters, bw, dl, jt, and er belong to QoS ones, and bwu, wlo, wbo, and fbo belong to resource utilization ones. Their quantitative models are described in Section 3.3.

To help understand our proposed scheme, we give a simple green multi-granularity transport network for illustration, shown in Fig. 2. We assume that there are two fibers on every link, four wavebands in every fiber, four wavelengths in every waveband, and the capacity of every wavelength is 10 Gbps. The parameter values are given directly, which in fact can be obtained as defined in Section 3.3.

3.2. Multiple many-to-many multicast requests

Based on the DiffServ model [39] and referring to ITU-T G.1010 [40], we assume that different types of applications are supported in the green multi-granularity transport networks in this paper, and $APS = \{AP_u | 1 \le u \le |APS|\}$ is the set of application types, where AP_u is an application type with QoS requirement QoS_u and $|APS|$ is the number of application types supported by the networks. Specifically, four QoS parameters, namely, bandwidth, delay, delay jitter, and error rate are considered, that is, $QoS_u = (\Delta bw_u, \Delta dl_u, \Delta jt_u, \Delta er_u)$, where $\Delta bw_u = [bw_u^{min}, bw_u^{max}]$, $\Delta dl_u = [dl_u^{min}, dl_u^{max}]$, $\Delta jt_u = [jt_u^{min}, jt_u^{max}]$ and $\Delta er_u = [er_u^{min}, er_u^{max}]$ represent the bandwidth, delay, delay jitter, and error rate requirements in terms of intervals respectively, and the bounds of the intervals are set based on ITU-T G.1010. Therefore, the flexible QoS [41] is supported in this paper.

We use $M^3R = \{M^2R^g | 1 \le g \le |M^3R|\}$ to denote multiple many-to-many multicast requests, where $|M^3R|$ is the number of many-to-many multicast requests M^2Rs in M^3R, of which traffic demands are known a prior with the same startup time. We use $M^2R^g =< MS^g, {AP_u}^g >$ to denote M^2Rs in M^3R, where $MS^g = \{{v_q}^g | {v_q}^g$ is a member in M^2R^g, which can act as the multicast source and sink, $1 \le q \le N\}$, and ${AP_u}^g \in APS$ is the application type of M^2R^g.

For example, we assume that there is a $M^3R = \{M^2R^1, M^2R^2\}$ in the illustrated network in Fig. 2; $M^2R^1 =< MS^1, {AP_3}^1 >, MS^1 = \{v_1^1, v_2^1, v_3^1\}, AP_3^1$ is video conference and its corresponding QoS_3=([384 kbps, 4 Mbps], [0, 400 ms], [0, 100 ms], [0, 0.01]); $M^2R^2 =< MS^2, AP_5^2 >, MS^2 = \{v_3^2, v_4^2, v_5^2\}$, AP_5^2 is cyber game and its corresponding QoS_5=([10 kbps, 10 Mbps], [0, 200 ms], [0, 40 ms], [0, 0]).

3.3. Quantitative models

In the following, we use Multiple Many-to-many Multicast Tree (M^3T) to denote a tree or trees corresponding to M^3R, Many-to-many Multicast Tree (M^2T^g) to denote the tree corresponding to M^2R^g in M^3R, $br_{s,d}^g$ to denote the branch between two members v_s^g and v_d^g in MS^g along M^2T^g.

From the power consumption aspect, at first we consider the power consumption $pc(v_i)$ of v_i. As shown in Fig. 1(a), it is the total power consumed by the active components, that is, the IP layer module, MG-MC-OXC, master engine, and optical transceivers in v_i. The power consumed by the IP layer module includes that consumed by active chassis, line cards, and ports; the power consumed by the MG-MC-OXC includes that consumed by active wavelength switching ports, waveband switching ports, fiber switching ports, multiplexers, de-multiplexers, and wavelength converters (if necessary). As shown in Fig. 1(b), the power consumption $pc(e_{i,j})$ of $e_{i,j}$ is the total power consumed by the active components, that is, active pre-amplifiers, in-line amplifiers, regenerators, and post-amplifiers in $e_{i,j}$. For details of node and link power consumption calculation, the reader can refer to our previous work [29]. The power consumption $pc(br_{s,d}^g)$

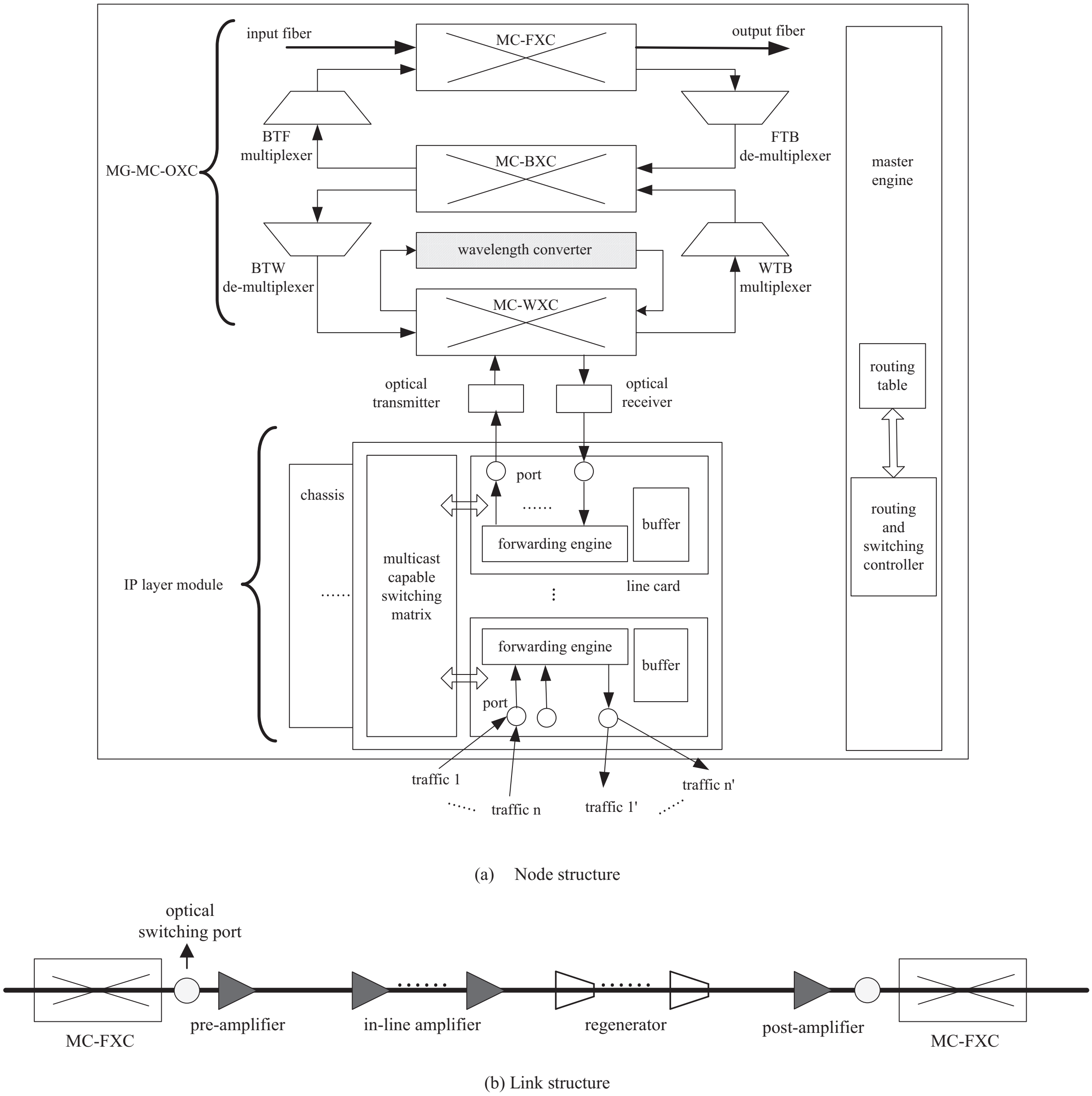

Fig. 1. Node and link structure in multi-granularity transport networks.

of $br^g_{s,d}$, $pc(M^2T^g)$ of M^2T^g, and $pc(M^3T)$ of M^3T are the total power consumed by the active components in nodes and links belonging to $br^g_{s,d}$, M^2T^g, and M^3T respectively. In addition, we use the average hop count hp from v_i to other members in the same MS as another power consumption related parameter. In fact, the small hp usually means the small amount of active components traversed by the traffics among these multicast members, leading to low power consumption.

From the QoS aspect, we use bw, dl, jt and er. The QoS of $br^g_{s,d}$ is calculated as follows:

$$bw(br^g_{s,d}) = min(bw(e_{i,j})), \quad \forall e_{i,j} \in br^g_{s,d} \tag{1}$$

$$dl(br^g_{s,d}) = \sum_{v_i \in br^g_{s,d}} dl(v_i) + \sum_{e_{i,j} \in br^g_{s,d}} dl(e_{i,j}), \tag{2}$$

$$jt(br^g_{s,d}) = \sum_{v_i \in br^g_{s,d}} jt(v_i) + \sum_{e_{i,j} \in br^g_{s,d}} jt(e_{i,j}), \tag{3}$$

$$er(br^g_{s,d}) = 1 - \prod_{v_i \in br^g_{s,d}} (1 - er(v_i)) \times \prod_{e_{i,j} \in br^g_{s,d}} (1 - er(e_{i,j})), \tag{4}$$

where v_i and $e_{i,j}$ are the node and link along $br^g_{s,d}$ respectively, $dl(v_i)$, $jt(v_i)$ and $er(v_i)$ are the delay, delay jitter and error rate of v_i respectively, $bw(e_{i,j})$, $dl(e_{i,j})$, $jt(e_{i,j})$ and

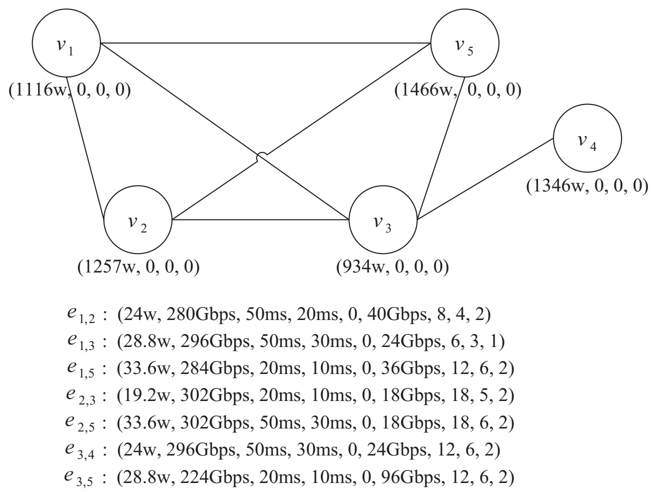

Fig. 2. A simple illustration example.

$er(e_{i,j})$ are the available bandwidth, delay, delay jitter and error rate of $e_{i,j}$ respectively.

The QoS of M^2T^g is calculated as follows:

$$bw(M^2T^g) = min\{bw(br^g_{s,d})\}, \quad \forall v^g_s, v^g_d \in MS^g \tag{5}$$

$$\delta(M^2T^g) = max\{\delta(br^g_{s,d})\}, \quad \forall v^g_s, v^g_d \in MS^g \tag{6}$$

where $bw(M^2T^g)$ is the available bandwidth of M^2T^g, δ is dl, jt or er and represents delay, delay jitter or error rate respectively.

In fact, the actual QoS values provided by a node or a link are heavily influenced by the amount of traffic load it transferred. How to derive them based on the traffic load is really complex and beyond the scope of this paper. We just assume that they could be got, for example, by the methods in [42, 43] or others.

From the resource utilization aspect, we use *bwu*, *wlo*, *wbo*, and *fbo*.

We can divide the above mentioned ten parameters into two types, that is, "the bigger the better" type and "the smaller the better" one. Among them, *bw* and *bwu* belong to the former, and the others belong to the latter. We define the exponential function based on the Efficacy Coefficient Method (*ECM*) [44] for each type of parameter, as shown in Eq. (7) and Eq. (8) respectively.

$$db(x) = \begin{cases} 1, & x > x_U \\ \exp\left(-\exp\left((x - x_U)/(x_L - x_U)\right)\right), & x_L \le x \le x_U \\ 0, & x < x_L \end{cases} \tag{7}$$

$$ds(x) = \begin{cases} 1, & x < x_L \\ 1 - \exp\left(-\exp\left((x - x_U)/(x_L - x_U)\right)\right), & x_L \le x \le x_U \\ 0, & x > x_U \end{cases} \tag{8}$$

We use them to evaluate the qualities of the actual values taken by these parameters with regard to the application requirements. Among them, x represents the parameter to be evaluated and is an independent variable; x_L and x_U represent the lower and upper bound of its value respectively and need to be determined according to the application type. In Eq. (7), $db(x)$ increases with x, and the bigger the value of the $db(x)$, the higher the quality of x is; when $x \ge x_U$, x attains its highest quality and the application requirement is satisfied completely, when $x \le x_L$, x gets its worst quality and the application requirement is totally dissatisfied. The situation of the Eq. (8) is just the opposite to that of Eq. (7). They are shown in Fig. 3(a) and (b) respectively.

Table 1
Bounds and notations for power consumption, QoS evaluation and resource utilization evaluation parameters.

parameter	x	x_L	x_U
pc	$pc(e_{i,j} + v_j)$	0	$pc(e + v)^{max}$
hp	$hp(v^g_j, MS^g)$	1	$2 \times MH^g$
bw	$bw(e_{i,j})$ or $bw(M^2T^g)$	bw^{min}_u	bw^{max}_u
dl	$dl(e_{i,j})$ or $dl(M^2T^g)$	dl^{min}_u	dl^{max}_u
jt	$jt(e_{i,j})$ or $jt(M^2T^g)$	jt^{min}_u	jt^{max}_u
er	$er(e_{i,j})$ or $er(M^2T^g)$	er^{min}_u	er^{max}_u
bwu	$bwu(e_{i,j})$	0	$TN_{bw}(e_{i,j})$
wlo	$wlo(e_{i,j})$	$RQ_{wl}(e_{i,j})$	$TN_{wl}(e_{i,j})$
wbo	$wbo(e_{i,j})$	$RQ_{wb}(e_{i,j})$	$TN_{wb}(e_{i,j})$
fbo	$fbo(e_{i,j})$	$RQ_{fb}(e_{i,j})$	$TN_{fb}(e_{i,j})$

The lower and upper bound of the considered parameters are given in Table 1. Here, $e_{i,j}$ represents a candidate link connecting v_i which has been chosen when routing and v_j which has not been chosen by that time; $pc(e_{i,j} + v_j)$ is the sum of the power consumption of $e_{i,j}$ and v_j; $pc(e + v)^{max}$ are the maximum of the sum of the power consumption of a link and its adjacent node in networks; $hp(v^g_j, MS^g)$ is the average hop count of v^g_j to other members in MS^g; MH^g is the maximum of the average hop count of each node to all other members in MS^g; $TN_{bw}(e_{i,j})$, $TN_{wl}(e_{i,j})$, $TN_{wb}(e_{i,j})$ and $TN_{fb}(e_{i,j})$ are the total bandwidth, the total number of wavelength, waveband, and fiber of $e_{i,j}$ respectively; $RQ_{wl}(e_{i,j})$, $RQ_{wb}(e_{i,j})$ and $RQ_{fb}(e_{i,j})$ are the number of the required wavelengths based on the already-in-use bandwidth of $e_{i,j}$, the number of the required wavebands based on the number of the already-in-use wavelengths of $e_{i,j}$, and the number of the required fibers

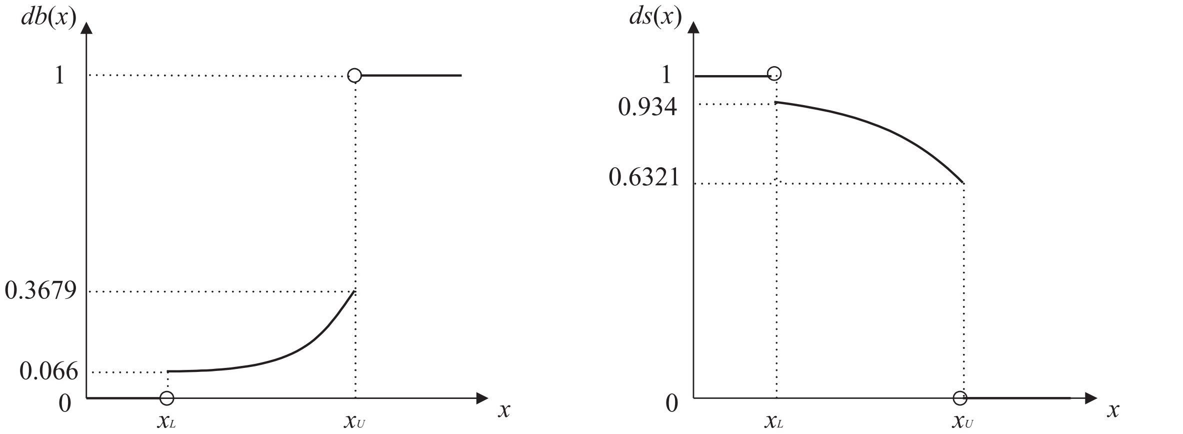

(a) Function of "the bigger the better'' type parameter (b) Function of "the smaller the better'' type parameter

Fig. 3. Illustration of the exponential functions.

based on the number of the already-in-use wavebands of $e_{i,j}$ respectively, which are calculated as follows:

$$RQ_{wl}(e_{i,j}) = \left\lceil \frac{bwu(e_{i,j})}{TN_{bw}(e_{i,j})/TN_{wl}(e_{i,j})} \right\rceil, \tag{9}$$

$$RQ_{wb}(e_{i,j}) = \left\lceil \frac{wlo(e_{i,j})}{TN_{wl}(e_{i,j})/TN_{wb}(e_{i,j})} \right\rceil, \tag{10}$$

$$RQ_{fb}(e_{i,j}) = \left\lceil \frac{wbo(e_{i,j})}{TN_{wb}(e_{i,j})/TN_{fb}(e_{i,j})} \right\rceil. \tag{11}$$

The evaluation on QoS of M^2T^g is defined as follows:

$$eq(M^2T^g) = w_u(bw) \times db\Big(bw\Big(M^2T^g\Big)\Big) + w_u(dl) \times ds\Big(dl\Big(M^2T^g\Big)\Big), + w_u(jt) \times ds\Big(jt\Big(M^2T^g\Big)\Big) + w_u(er) \times ds\Big(er\Big(M^2T^g\Big)\Big) \tag{12}$$

where $w_u(bw)$, $w_u(dl)$, $w_u(jt)$ and $w_u(er)$ are the weights of bandwidth, delay, delay jitter and error rate for AP_u^g respectively, which represent the relative importance of different QoS parameters to the application, $0 < w_u(bw)$, $w_u(dl)$, $w_u(jt)$, $w_u(er) < 1$, and $w_u(bw) + w_u(dl) + w_u(jt) + w_u(er) = 1$. Their values can be set by user experiences, experiments, or Analytic Hierarchy Process (AHP) with triangular fuzzy number or other ways [45].

For each M^2R^g in M^3R, we obtain $eq(M^2T^g)$ on its corresponding M^2T^g. Then, we can get the average value of all $eq(M^2T^g)$s and their variance, denoted as *avg_eq* and *var_eq* respectively. Then, we define the evaluation on QoS of M^3T as follows:

$$eq(M^3T) = avg\_eq^{var\_eq}. \tag{13}$$

Apparently, $eq(M^3T)$ increases with the increment of *avg_eq* and with the decrement with *var_eq*; the bigger the value of *avg_eq* and the smaller the value of *var_eq*, the bigger the value of $eq(M^3T)$, and then the higher the quality of M^3T. In fact, we encourage that not only should all M^2R^g in M^3R get high QoS but also they should be treated equally.

The evaluation on resource utilization of $e_{i,j}$ is defined as follows:

$$eu(e_{i,j}) = \frac{db(bwu(e_{i,j})) + ds(wlo(e_{i,j})) + ds(wbo(e_{i,j})) + ds(fbo(e_{i,j}))}{4}. \tag{14}$$

Apparently, for each link, the more its bandwidth-in-use at the same time the less its wavelength-in-use, its waveband-in-use and its fiber-in-use, then the better its resource utilization. For each $e_{i,j}$ in M^3T, we obtain its $eu(e_{i,j})$, then we can get the average value of all $eu(e_{i,j})$s and their variance, denoted as *avg_eu* and *var_eu* respectively. We define the evaluation on resource utilization of M^3T as follows:

$$eu(M^3T) = avg\_eu^{var\_eu}. \tag{15}$$

The properties of $eu(M^3T)$ are similar to those of $eq(M^3T)$.

3.4. Problem definition

The proposed *PQRS* in this paper tries to build tree or trees for multiple many-to-many multicast requests with power consumption minimized, QoS evaluation and resource utilization evaluation maximized under multiple constraints. Its mathematical description is as follows:

$$\text{Minimize} \quad pc(M^3T) \tag{16}$$

$$\text{Maximize} \quad eq(M^3T) \tag{17}$$

$$\text{Maximize} \quad eu(M^3T) \tag{18}$$

$$\text{s.t.}\, S_{ch}^{k}(v_i) \le \sum_{l=1}^{N_{lc}^{k}(v_i)} S_{lc}^{k,l}(v_i), \quad \forall i, k, l \tag{19}$$

$$S_{lc}^{k,l}(v_i) \le \sum_{p=1}^{N_{pt}^{k,l}(v_i)} S_{pt}^{k,l,p}(v_i), \quad \forall i, k, l, p \tag{20}$$

$$S_{ch}^{k}(v_i) \ge S_{lc}^{k,l}(v_i), \quad \forall i, k, l \tag{21}$$

Table. 2
Notations used in constraints (19)–(27).

Name	Description
$S_{ch}^{k}(v_i)$	The status of the kth chassis in the IP layer at v_i
$S_{lc}^{k,l}(v_i)$	The status of the lth line card of the kth chassis in the IP layer at v_i
$S_{pt}^{k,l,p}(v_i)$	The status of the pth port of the lth line card of the kth chassis in the IP layer at v_i
$N_{lc}^{k}(v_i)$	The number of line cards of the kth chassis at v_i
$N_{pt}^{k,l}(v_i)$	The number of ports of the lth line card of the kth chassis at v_i
$C(e_{i,j})$	Capacity of $e_{i,j}$
$C^{fb}(e_{i,j})$	Capacity of a fiber on $e_{i,j}$
$C^{fb,wb}(e_{i,j})$	Capacity of a waveband in a fiber on $e_{i,j}$
BW^{fb}	Bandwidth allocated to a fiber
BW^{wb}	Bandwidth allocated to a waveband
BW^{wl}	Bandwidth allocated to a wavelength

$$S_{lc}^{k,l}(v_i) \geq S_{pt}^{k,l,p}(v_i), \quad \forall i, k, l, p \tag{22}$$

$$\sum_{fb \in e_{i,j}} BW^{fb} \leq C(e_{i,j}), \quad \forall e_{i,j} \tag{23}$$

$$\sum_{wb \in fb} BW^{wb} \leq C^{fb}(e_{i,j}), \quad \forall e_{i,j}, \ \forall fb \in e_{i,j} \tag{24}$$

$$\sum_{wl \in wb} BW^{wl} \leq C^{fb,wb}(e_{i,j}), \quad \forall e_{i,j}, \ \forall fb \in e_{i,j}, \ \forall wb \in fb \tag{25}$$

$$bw(M^2T^g) \geq bw_u^{min}, \quad 1 \leq g \leq \left|M^3R\right| \tag{26}$$

$$\delta(M^2T^g) \leq \delta_u^{max}, \quad 1 \leq g \leq \left|M^3R\right| \tag{27}$$

The notations in constraints (19) - (27) are defined in Table 2. Here, $S_{ch}^{k}(v_i)$, $S_{lc}^{k,l}(v_i)$ and $S_{pt}^{k,l,p}(v_i)$ denote the status of chassis, line card and port in v_i respectively, where 0 means idle and 1 means active. Constraint (19) guarantees that the number of active chassis does not exceed the number of active line cards, constraint (20) guarantees that the number of active line cards does not exceed the number of active ports, constraint (21) guarantees that a chassis is active as long as there is any active line card on it, and constraint (22) guarantees that a line card is active as long as there is any active port on it. Constraints (23)-(25) guarantee that the bandwidth allocated to a fiber, a waveband or a wavelength does not exceed the capacity of the corresponding link, fiber, or waveband respectively. Constraint (26) guarantees that the bandwidth of M^2T^g is not lower than the lower bound of the corresponding requirement interval of AP_u^g. Constraint (27) guarantees that the delay, delay jitter, and error rate of M^2T^g do not exceed the upper bounds of the corresponding requirement intervals of AP_u^g.

The above problem is a multi-constrained multi-objective optimization one. According to [46] and [47], the well-known routing and wavelength assignment (RWA) problem in optical WDM networks and QoS multicast routing problem in IP networks are NP-complete, and their mathematic formulations are the subsets of that of the problem to be solved in this paper. Under more constraints to be followed and with more objectives to be optimized, it is more complex mathematically than the problems in [46] and [47], and thus we propose a heuristic algorithm for it to find feasible solutions.

4. Algorithm description

4.1. Basic idea

The proposed routing scheme in this paper is oriented to the green multi-granularity transport networks. We have to deal with both the IP layer and the optical layer with various components (such as fiber, waveband, wavelength, transceiver, port, line card, chassis, etc.) in nodes and links considered. It is too hard to deal with all the above aspects only over the physical network topology; therefore we construct the LAG based on the physical topology to solve the routing problem for M^3R in an integrated way. According to the proposed node structure and link structure in this paper, there are eight layers in our proposed LAG, that is, access layer, chassis layer, line card layer, port layer, transceiver layer, wavelength layer, waveband layer, and fiber layer, from the bottom to top. The edge's weight represents its capacity, power consumption, delay, delay jitter, and error rate. For the details of the LAG construction, the reader can refer to [29].

Over the constructed LAG, we build M^3T for M^3R. The basic idea of the proposed scheme is described as follows. For M^3R, at first a One-to-many Multicast Tree (*OMT*) is built for each member in each M^2R^g with the member as the root of the *OMT*, and those links which help save power consumption, increase QoS evaluation and improve resource utilization evaluation are preferred based on our proposed *CPM* (see details in Section 4.2). Then, an M^2T^g is built for each M^2R^g by merging all *OMT*s of its members. Finally, M^3T is built for M^3R by merging all M^2T^gs corresponding to those M^2R^gs, during which our devised multiplexing phase is carried out to optimize the merging process by promoting reusing the same active components as many as possible and thus help save power further.

4.2. Chosen probability model

We define the Chosen Probability (*CP*) of a link when routing is done as Eq. (28).

Apparently, *CP* is the geometric mean of the involved ten parameters, that is, the tenth root of the product of $ds(pc)$, $ds(hp)$, $db(bw)$, $ds(dl)$, $ds(jt)$, $ds(er)$, $db(bwu)$, $ds(wlo)$, $ds(wbo)$, and $ds(fbo)$. A bigger *CP* means that the corresponding link should have lower power consumption, higher QoS evaluation and better resource utilization evaluation than the smaller one. Thus, a link with the biggest *CP* among candidates should be chosen when building an *OMT*.

The procedure of calculating the *CP* of a candidate link when a multicast member builds the *OMT* is described in Algorithm 1. Its inputs are LAG, M^2R^g, U, and $e_{i,j}$; its output is the chosen probability of $e_{i,j}$ by the nodes in U and is denoted as $CP(e_{i,j}, U)$, U denotes the set of nodes which have been chosen when building an *OMT*, and $e_{i,j}$ connects v_i in U and v_j in V-U.

and G from which LAG is constructed, and its output is M^3T or 0 (i.e., the solution cannot be found).

$$CP=\sqrt[10]{ds(pc(e_{i,j}+v_j))\times ds(hp(v_j,\ MS^g))\times db(bw(e_{i,j}))\times ds(dl(e_{i,j}))\times ds(jt(e_{i,j}))\times ds(er(e_{i,j}))\times db(bwu(e_{i,j}))\times ds(wlo(e_{i,j}))\times ds(wbo(e_{i,j}))\times ds(fbo(e_{i,j}))} \quad (28)$$

In Algorithm 1, lines 1-2 are to calculate the power consumption evaluation value. Lines 3-8 are to calculate the hop count evaluation value based on whether the candidate node is a multicast member. Line 9 is to calculate the QoS evaluation value. Lines 10-13 are to calculate the resource utilization evaluation value. Line 14 is to calculate the chosen probability of a link.

Recall the illustration example in Section 3.1, let us consider $e_{1,2}$ in Fig. 2. We assume that two fibers are occupied, two wavebands are occupied in each occupied fiber, two wavelengths are occupied in each occupied waveband, and 5 Gbps is used in each occupied wavelength. Then, we can calculate the *CP* of $e_{1,2}$ selected by a multicast member, for example, v_1^1 in M^2R^1. Here, $pc(e_{1,2}) = 24w$, $pc(v_2) = 1257w$, $pc(e_{1,2}+v_2)_L = 0$, $pc(e_{1,2}+v_2)_U = pc(e+v)^{max} = 1499.6w$, then $ds(pc(e_{1,2}+v_2)) = 0.6855$ by Eq. (8); $v_2^1 \in MS^1$, the average hop count of v_2^1 to the other members in MS^1 is 1, that is, $hp(v_2^1,\ MS^1) = 1$, $hp(v_2^1,\ MS^1)_L = 1$, $hp(v_2^1,\ MS^1)_U = 2 \times MH^g = 2$, thus $ds(hp(v_2^1, MS^1)) = 0.934$ by Eq. (8); $bw(e_{1,2}) = 280$ Gbps, $bw(e_{1,2})_L = bw(e_{1,2})_3^{min} = 0.384$ Mbps, $bw(e_{1,2})_U = bw(e_{1,2})_3^{max} = 4$ Mbps, thus $db(bw(e_{1,2})) = 1$ by Eq. (7); $dl(e_{1,2}) = 50$ ms, $dl(e_{1,2})_L = dl(e_{1,2})_3^{min} = 0$, $dl(e_{1,2})_U = dl(e_{1,2})_3^{max} = 400$ ms, thus $ds(dl(e_{1,2})) = 0.9091$ by Eq. (8); $jt(e_{1,2}) = 20$ ms, $jt(e_{1,2})_L = jt(e_{1,2})_3^{min} = 0$, $jt(e_{1,2})_U = jt(e_{1,2})_3^{max} = 100$ ms, thus $ds(jt(e_{1,2})) = 0.8919$ by Eq. (8); $er(e_{1,2}) = 0$, $er(e_{1,2})_L = er(e_{1,2})_3^{min} = 0$, $er(e_{1,2})_U = er(e_{1,2})_3^{max} = 0.01$, thus $ds(er(e_{1,2})) = 0.934$ by Eq. (8); $bwu(e_{1,2}) = 40$ Gbps, $bwu(e_{1,2})_L = 0$, $bwu(e_{1,2})_U = TN_{bw}(e_{1,2}) = 320$ Gbps, thus $db(bwu(e_{1,2})) = 0.0909$ by Eq. (7); $wlo(e_{1,2}) = 8$, $wlo(e_{1,2})_L = RQ_{wl}(e_{1,2}) = 4$, $wlo(e_{1,2})_U = TN_{wl}(e_{1,2}) = 32$, thus $ds(wlo(e_{1,2})) = 0.9052$ by Eq. (8); $wbo(e_{1,2}) = 4$, $wbo(e_{1,2})_L = RQ_{wb}(e_{1,2}) = 2$, $wbo(e_{1,2})_U = TN_{wb}(e_{1,2}) = 8$, thus $ds(wbo(e_{1,2})) = 0.8574$ by Eq. (8); $fbo(e_{1,2}) = 2$, $fbo(e_{1,2})_L = RQ_{fb}(e_{1,2}) = 1$, $fbo(e_{1,2})_U = TN_{fb}(e_{1,2}) = 2$, thus $ds(fbo(e_{1,2})) = 0.6321$ by Eq. (8); finally, $CP(e_{1,2},\ \{v_1^1\})$ is 0.6815 by Eq. (28).

4.3. Heuristic routing algorithm

Existing algorithms, which are discussed in Section 2, and well-known ones, for example *PRIM*, cannot be used directly to deal with both IP layer and optical layer over the LAG in an integrated way in multi-granularity transport networks, especially when routing, they do not consider to optimize power saving, QoS evaluation enhancement and resource utilization evaluation improvement under QoS and capacity constraints, in addition, they are not purposely designed for multiple many-to-many multicast requests with given static traffic demands, thus we devise a new algorithm for the problem to be solved in this paper. Due to its NP-completeness, we propose a heuristic algorithm, which is called *RCPM*, to build the optimized M^3T for M^3R based on the *CPM*. We describe *RCPM* in Algorithm 2. Its inputs are M^3R and G from which LAG is constructed, and its output is M^3T or 0 (i.e., the solution cannot be found).

In Algorithm 2, lines 3-17 are to build an *OMT* for each member in MS^g, among them, lines 6-8 are to calculate the *CP* of each candidate link with Algorithm 1, lines 12–14 are to determine whether all members in MS^g are covered. Lines 18-20 are to generate M^2T^g for its corresponding M^2R^g; because T^g is generated by merging the $|MS^g|$ number of *OMTs* and thus may have loops and redundant branches which do not cover any multicast members, we have to make it loop free without useless branches to M^2T^g. Lines 21-23 are to determine whether the M^2T^g satisfy the QoS constraints of its corresponding M^2R^g. Lines 25-28 are to generate M^3T by merging M^2T^g with the so-called multiplexing phase carried out, trying to make M^3R traffics transfer along the same routes and use the same active components as many as possible. Lines 30-32 are to see whether the generated M^3T satisfies the capacity constraints.

The time complexity of the Algorithm 2 is $O(|M^3R| \times |MS^g| \times N^3 + |M^3R| \times N^2 \times W) = O(N^5 + W \times N^3)$, where W is the maximum of the number of wavelengths in a waveband which is denoted as $N_{wl}(wb)$, the number of wavebands in a fiber which is denoted as $N_{wb}(fb)$, and the number of fibers in a link which is denoted as N_{fb}, that is, $W = max(N_{wl}(wb),\ N_{wb}(fb),\ N_{fb})$.

For $M^3R = \{M^2R^1,\ M^2R^2\}$ in Section 3.2, at first we build three *OMTs* for $\{v_1^1,\ v_2^1,\ v_3^1\}$ in M^2R^1 and three *OMTs* for $\{v_3^2,\ v_4^2,\ v_5^2\}$ in M^2R^2. As an example, we illustrate how to build an *OMT* for v_1^1 as follows. In the beginning, there is only one node, that is, v_1^1, in the tree, as shown in Fig. 4(a). Next, we calculate the *CP* of every candidate link and get $CP(e_{1,2},\ \{v_1^1\})$, $CP(e_{1,3},\ \{v_1^1\})$, and $CP(e_{1,5},\ \{v_1^1\})$ which are 0.6815, 0.7093, and 0.6557 respectively, thus we choose $e_{1,3}$ because it has the maximum *CP*, and put $e_{1,3}$ and v_3^1 into the tree, as shown in Fig. 4(b). After that, we calculate the *CP* of all candidate links $\{e_{1,2},\ e_{1,5},\ e_{3,2},\ e_{3,4},\ e_{3,5}\}$ for $\{v_1^1,\ v_3^1\}$ and choose $e_{3,5}$ due to its maximum *CP*, putting $e_{3,5}$ and v_5 into the tree, as shown in Fig. 4(c). We proceed to calculate the *CP* of all candidate links $\{e_{1,2},\ e_{3,2},\ e_{3,4},\ e_{5,2}\}$ for $\{v_1^1,\ v_3^1,\ v_5\}$ and choose $e_{3,2}$ due to its maximum *CP*, putting $e_{3,2}$ and v_2^1 into the tree, as shown in Fig. 4(d). By this time, we have generated a tree covering all multicast members in MS^1 from v_1^1, however, since v_5 does not belong to MS^1, we cut down $e_{3,5}$ from the generated tree and get the *OMT* for v_1^1 as shown in Fig. 4(e). We build two other *OMTs* with v_2^1 and v_3^1 as their roots respectively in the same way as the above, as shown in Fig. 4(f) and (g). Then, we construct M^2T^1 for M^2R^1 by merging these three *OMTs*, as shown in Fig. 4(h). Similarly, we construct M^2T^2 for M^2R^2 as shown in Fig. 4(i). Finally, we merge M^2T^1 and M^2T^2 with the devised multiplexing phase applied, and get M^3T shown in Fig. 4(j).

5. Simulation study

5.1. Experimental setting

We use Microsoft Visual Studio 2010 to simulate our proposed *PQRS* and compare it with the devised Many-to-Many

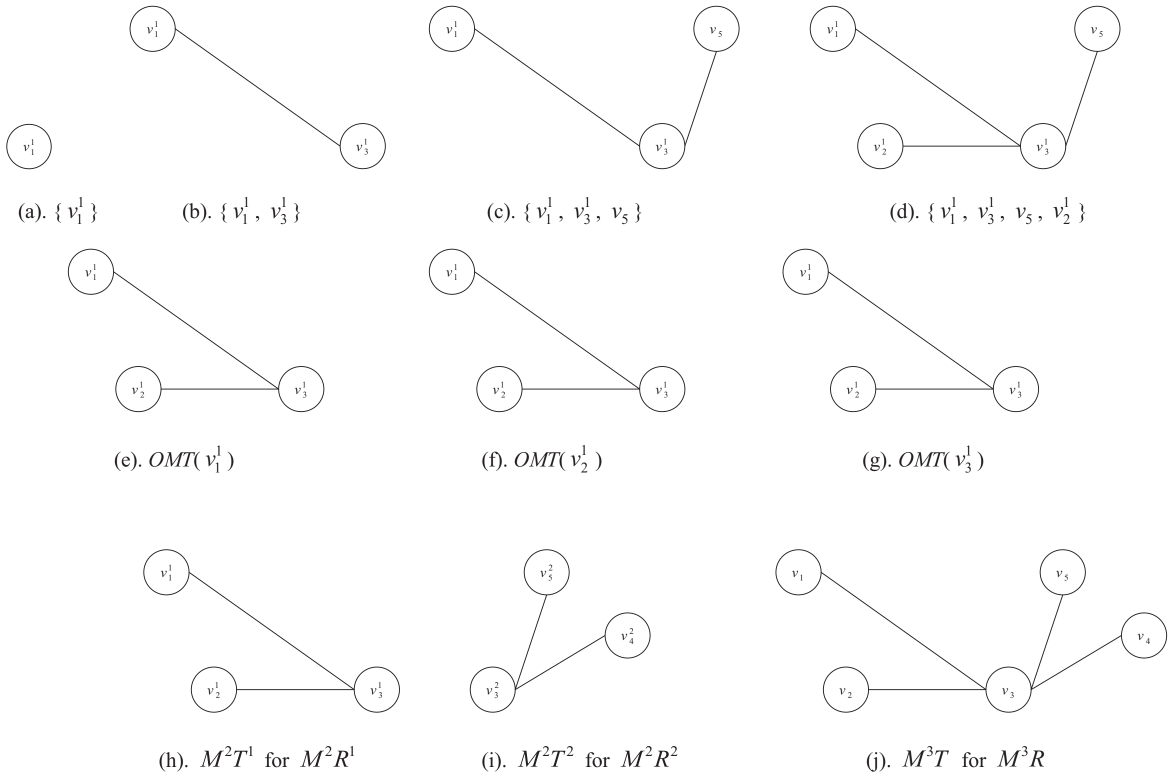

Fig. 4. Illustration of M^3T for M^3R.

Table. 3
Network parameter values used in simulation.

Parameter	Value
Capacity of a wavelength	10 Gbps
Average number of members in a multicast request	8
Number of chassis at every node	4
Number of line cards on a chassis at every node	4
Number of ports on a line card of a chassis at every node	4
Number of wavelengths in a waveband	4
Number of wavebands in a fiber	5
Number of fibers in a link	6

Table. 4
Power consumption parameter values used in simulation.

Parameter	Value
Energy consumption of a port in IP layer module	150 W
Energy consumption of a wavelength, a waveband or a fiber witching port in MG-MC-OXC	20 W
Energy consumption of a multiplexer or a de-multiplexer in MG-MC-OXC	1 W
Energy consumption of a master engine	356 W
Energy consumption of an optical transceiver	3.5 W
Energy consumption of a wavelength converter	18 W
Energy consumption of an optical pre-amplifier, an in-line amplifier or a post-amplifier	4.8 W
Energy consumption of an optical regenerator	26 W

Multi-hop Bypass Heuristic Approach (*MM-MBHA*) based on *MBHA* [48] and the well-known *PRIM* algorithm [49]. *MBHA* is a heuristic method based on the lightpath bypass strategy for the IP over WDM networks. It firstly orders all the node pairs based on their traffic demands from the highest to the lowest volume, and builds a virtual topology (*VG*) over the physical topology. Then it routes the traffic demand of every node pair over *VG* in turn. If there is sufficient capacity over *VG*, the request is accommodated; otherwise, a new direct virtual link is established to allocate the necessary capacity to the request. It finally routes all the virtual links on *VG* over the physical topology in the optical layer. *MBHA* not only takes IP and optical layers into account in an integrated way, but also routes over a virtual topology. However, it is oriented to unicast scenario, thus in our devised *MM-MBHA*, each many-to-many multicast request is handled as multiple unicast requests among multicast members, then routes for these unicast requests are found by *MBHA*, finally merge these routes to get the solution for M^3R.

The simulation topologies are NSFNET of USA, GéANT2 of Europe, SINET4 of Japan, and CERNET2 of China as shown in Fig. 5(a)-(d) respectively. The network parameter values used in simulation are set as in Table 3. By referring to Cisco CRS-3 [50] and Cisco ONS 15454 [51], the power consumption parameter values used in simulation are set as in Table 4. The configurations of the computer used for simulation are as follows: Intel Core i3-4150 @ 3.50 GHz Dual Core, RAM 4 GB (DDR3, 1600 MHz), Windows 8.1 professional 64 bit.

We use the following metrics to do performance evaluation and comparison: *Network Power Consumption* (*NPC*), i.e., the total power consumed by all devices in networks due to M^3R; *Routing Success Ratio* (*RSR*), i.e., the ratio of the

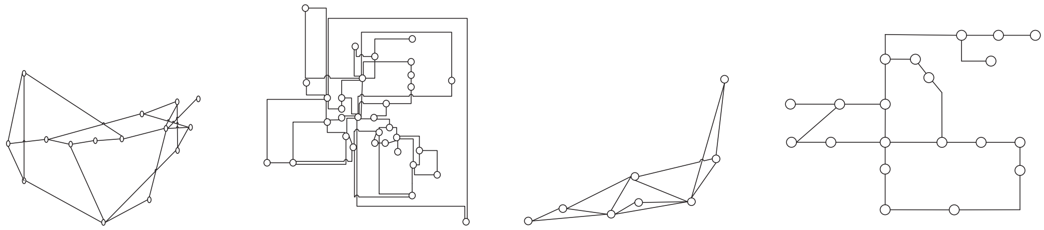

(a) NSFNET (b) GéANT2 (c) SINET4 (d) CERNET2

Fig. 5. Network topologies used in simulation.

Algorithm 1
Calculate $CP(e_{i,j}, U)$.

Input: LAG, M^2R^g, U, and $e_{i,j}$
Output: $CP(e_{i,j}, U)$
Calculate $pc(e_{i,j}+v_j)$ and $pc(e+v)^{max}$;
Calculate $ds(pc(e_{i,j}+v_j))$;
if $v_j \in MS^g$ **then**
  Get $hp(v_j^g, MS^g)$;
  Calculate $ds(hp(v_j^g, MS^g))$;
else
  $ds(hp(v_j, MS^g)) = ds(2 \times MH^g)$;
end if
Calculate $db(bw(e_{i,j}))$, $ds(dl(e_{i,j}))$, $ds(jt(e_{i,j}))$, and $ds(er(e_{i,j}))$;
Calculate $bwu(e_{i,j})$ and $TN_{bw}(e_{i,j})$;
Calculate $db(bwu(e_{i,j}))$;
Calculate $\gamma o(e_{i,j})$, $RQ_\gamma(e_{i,j})$, and $TN_\gamma(e_{i,j})$ (γ denotes *wl*, *wb* and *fb*);
Calculate $ds(\gamma o(e_{i,j}))$;
Calculate $CP(e_{i,j}, U)$;
Return $CP(e_{i,j}, U)$.

Algorithm 2
RCPM

Input: G, M^3R
Output: M^3T or 0
Cut down the links in *G*, which does not satisfy the QoS requirements of M^3R, and then build LAG.
for each $M^2R^g \in M^3R$ **do**
  for each $v_q^g \in MS^g$ **do**
    $U = \{v_q^g\}$;
    while $U \neq V$ **do**
      for each candidate link $e_{i,j}$ between any v_i in *U* and any v_j in *V-U* **do**
      Calculate $CP(e_{i,j}, U)$ with Algorithm 1;
      end for
      Choose the link with the maximum *CP*;
      Get the corresponding candidate node v_j;
      $U = U \cup \{v_j\}$;
      if $MS^g \subseteq U$ **then**
      Break;
      end if
    end while
    Prune those redundant branches which do not cover any multicast members in MS^g and get the *OMT* of which root is v_q^g;
  end for
  Merge all *OMT*s, which are corresponding to the M^2R^g, into T^g;
  Make T^g loop-free and prune all redundant branches by deleting those useless links, especially deleting those with smaller *CP*s than others whenever possible;
  Get the M^2T^g;
  if Constraints (26)–(27) are not satisfied by the M^2T^g **then**
  Return 0;
  end if
end for
Merge all M^2T^gs;
for any overlapped segments among M^2T^gs **do**
  Multiplex the same already-in-use wavelengths, wavebands, fibers and other active components along them as long as they have enough capacities to accommodate all their transferred traffics from M^3R;
  Release all no-longer-needed wavelengths, wavebands, fibers and other active components;
end for
Get M^3T;
if Constraints (19)–(25) are not satisfied by M^3T **then**
  Return 0;
end if
Return M^3T.

number of M^3Rs successfully accommodated by the network to the total number of M^3Rs received by the network; *Resource Utilization Ratio* (*RUR*), that is, *bwur, wlor, wbor,* and *fbor,* which represent the ratio of the already-in-use bandwidth to the total bandwidth, the ratio of the number of the already-in-use wavelengths to the total number of the wavelengths, the ratio of the number of the already-in-use wavebands to the total number of the wavebands, and the ratio of the number of the already-in-use fibers to the total number of the fibers respectively; *Average Running Time* (*ART*), i.e., the average time for the proposed routing scheme used from the time point of M^3R received to the time point of M^3T built.

5.2. Comparison with MM-MBHA

In Fig. 6, we compare the results of *NPC* of *PQRS* and *MM-MBHA* over four different topologies. In each topology, the number of M^2Rs in M^3R increases from 2 to 10. As the number of M^2Rs increases, the power consumption also increases smoothly. However, when it increases to a critical value, for example, 8 in Fig. 6(a), most devices are already active and thus the increasing rate of power consumption decreases, leading to a convergence trend. If it continues to increase, the power consumption becomes saturated. The comparison results of the two schemes show that the power consumed by *PQRS* is much lower than *MM-MBHA*. Therefore, *PQRS* is more power-efficient than *MM-MBHA*.

To verify the effectiveness of *CPM*, we integrate it with *MM-MBHA*. As shown in Fig. 6, the power consumption of *MM-MBHA* with *CPM* (*MM-MBHA-CPM*) is less than *MM-MBHA* over the four topologies. This is because *CPM* could help to find routes with lower power consumption between

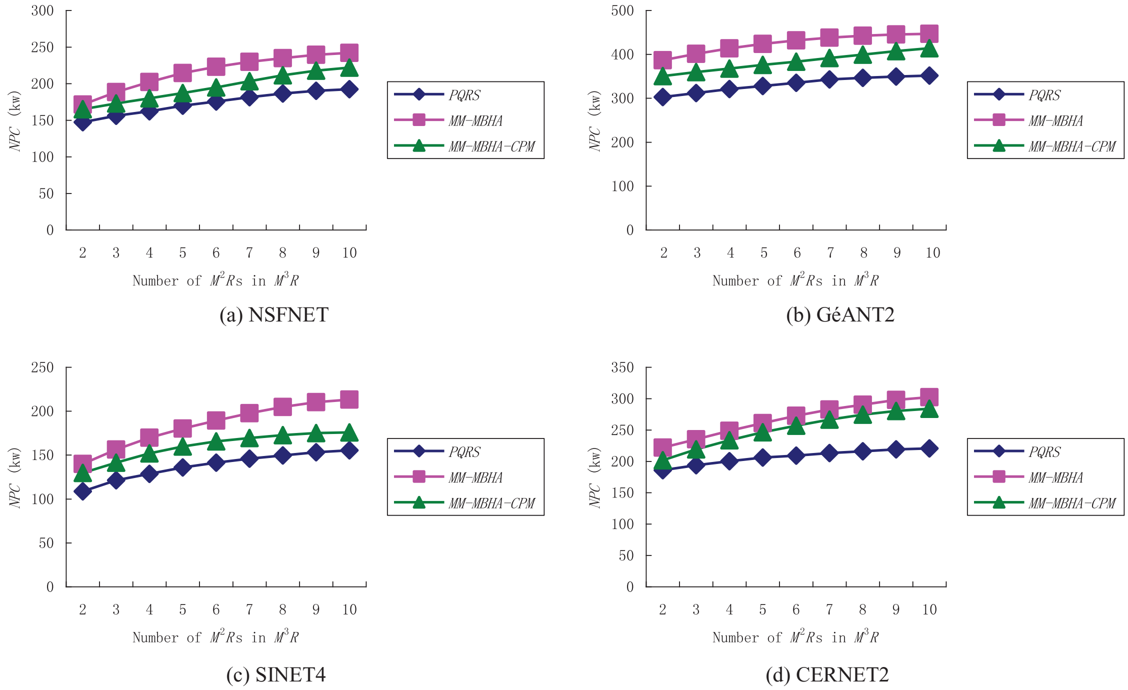

Fig. 6. Comparison of *NPC* among *PQRS*, *MM-MBHA* and *MM-MBHA-CPM*.

node pairs. However, the power consumption of *MM-MBHA-CPM* is still higher than *PQRS*. The reason is that *MM-MBHA-CPM* lacks the multiplexing phase of *PQRS* and thus occupies more resources, leading to more active components and higher power consumption.

As shown in Fig. 6, the above three schemes have produced significantly different *NPC* over the four topologies. The reason is due to the fact that the four topologies have different sizes. SINET4 only has 8 nodes and 13 links, NSFNET has 15 nodes and 22 links, CERNET2 has 20 nodes and 22 links, and GéANT2 has 33 nodes and 50 links. Since M^3Rs are randomly generated when doing simulation, the corresponding M^3Ts in larger networks often traverse more nodes and links than their counterparts in smaller ones. Therefore, the M^3Ts built in SINET4 consume the least power among the four topologies, while the M^3Ts built in GéANT2 consume the most power.

As shown in Fig. 7, the higher *RSR* of *PQRS* than that of *MM-MBHA* and *MM-MBHA-CPM* demonstrates the effectiveness of considering QoS requirements when routing. While in *MM-MBHA*, there are more routes which could be found, but their probabilities of satisfying QoS constraints are low. The *RSR* of *MM-MBHA-CPM* is better than that of *MM-MBHA*, because the former uses *CPM* and tries to select links with higher *CPs* to satisfy QoS requirements and improve QoS evaluation when routing. However, with the increase of the number of M^2Rs, the available resource becomes less and less, and then the *RSR* decreases. In addition, we can see from Fig. 7 that the three schemes have produced significantly different *RSRs* over the four topologies. The reason is that they have different average node degrees (SINET4 1.625, NSFNET 1.467, CERNET2 1.1, and GéANT2 1.515). The higher average node degree usually provides the node more choice when routing, leading to the higher *RSR*. Therefore, the M^3Ts built in SINET4 get the highest *RSR*, while the M^3Ts built in CERNET2 usually get the lowest *RSR*.

To demonstrate the *RUR* of *PQRS*, *MM-MBHA* and *MM-MBHA-CPM* over the four topologies, we choose the following two scenarios: 4 M^2Rs in M^3R and 8 M^2Rs in M^3R. As shown in Fig. 8, we observe that *fbo* is the highest, *bwu* is the lowest, *wlo* and *wbo* are between *fbo* and *bwu*. The reason is that fiber and bandwidth are the coarsest and finest resource allocation granularity respectively with wavelength and waveband between them, and then, for example, *wbo* is equal to *fbo* only when all wavebands of the occupied fibers of the link are occupied. We also observe that the performance of *PQRS* is better than that of *MM-MBHA* and *MM-MBHA-CPM*, this is because the multiplexing phase of *PQRS* makes its *wlo* and *wbo* be significantly improved. The better *RUR* implies the higher *bwu* and the lower *wlo*, *wbo* and *fbo*, and the lower *wlo*, *wbo* and *fbo* implies the less power consumption. Moreover, as the number of M^2Rs increases, the *RUR* increases to 1 gradually. Fig. 8 also shows that the three schemes have produced significantly different *RUR* over the four topologies. The larger network often has more resources than the smaller one, thus under the same traffics, all three schemes get higher *bwu*, *wlo*, *wbo* and *fbo* in smaller networks than in larger ones.

In Fig. 9, we compare the *ART* of *PQRS*, *MM-MBHA* and *MM-MBHA-CPM* over the four topologies. We observe that the *ART* of *PQRS* is longer than that of *MM-MBHA* and *MM-MBHA-CPM*. As mentioned previously, in generating a *OMT* for each multicast member in each M^2R, *PQRS* calculates the *CP* for each candidate link, while *MM-MBHA* only finds routes for requests between node pairs orderly from the highest to the lowest traffic volume. Although *MM-MBHA-CPM*

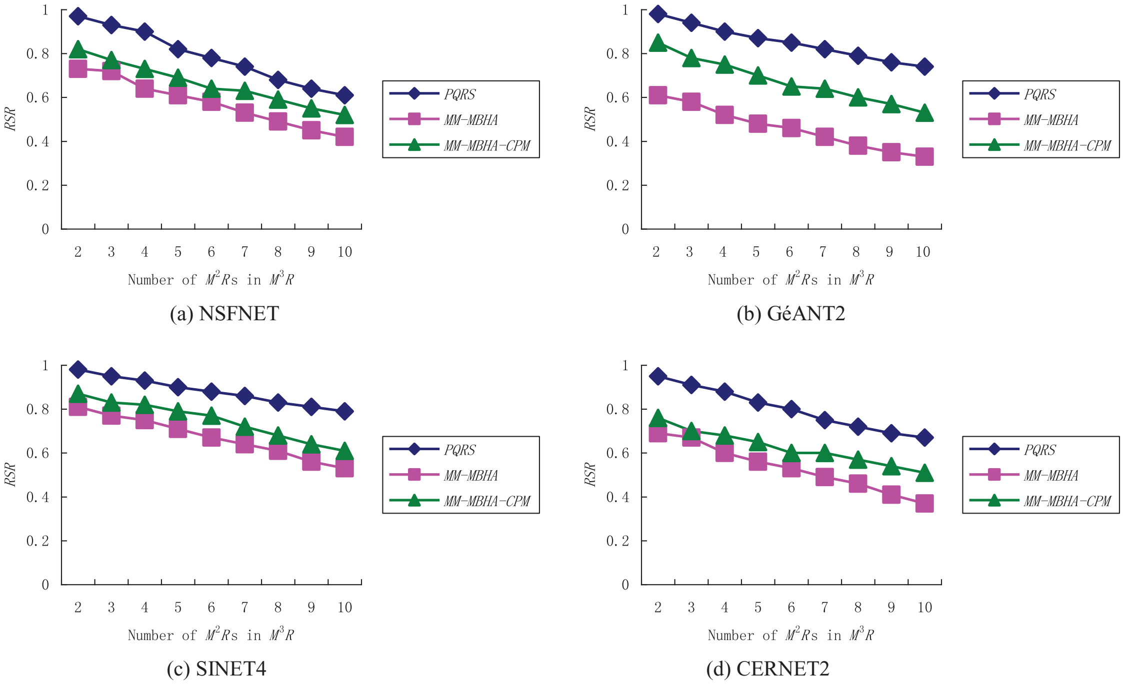

Fig. 7. Comparison of *RSR* among *PQRS*, *MM-MBHA* and *MM-MBHA-CPM*.

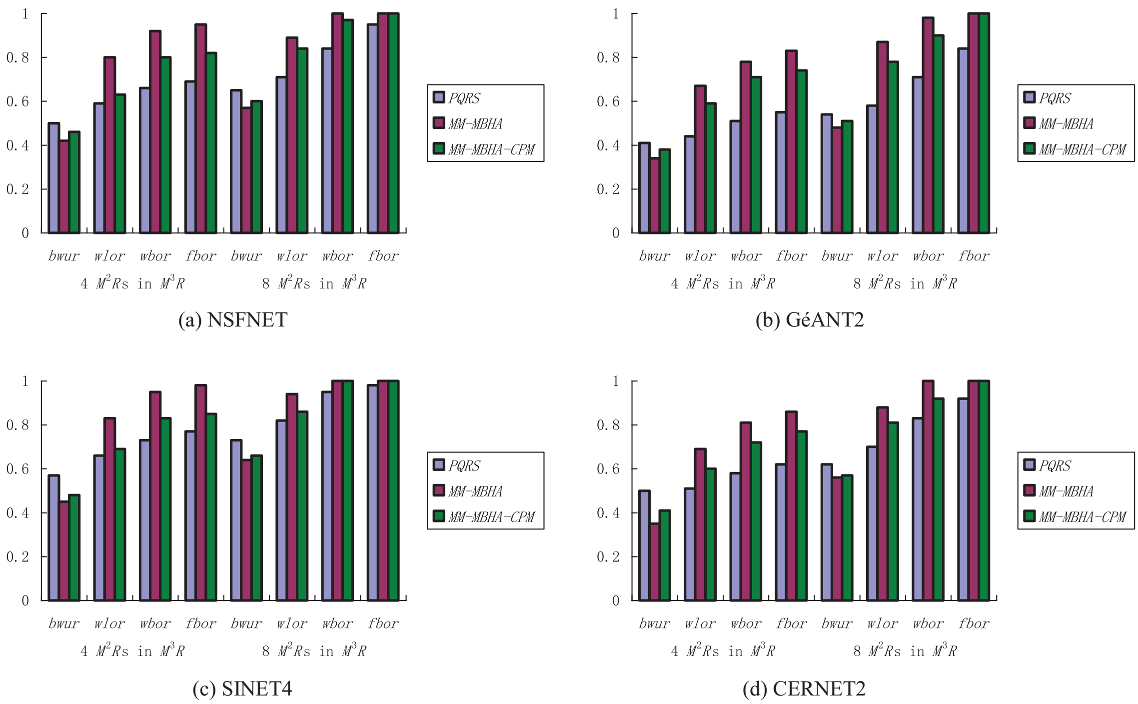

Fig. 8. Comparison of *RUR* among *PQRS*, *MM-MBHA* and *MM-MBHA-CPM*.

computes the *CP* for links, however, it does not have the multiplexing phase as in *PQRS* and hence it consumes less time than *PQRS*. As shown in Fig. 9, with the increase of the number of M^2Rs, the *ART* increases sharply due to significant increment of computation. Fig. 9 also shows that with the network size increases, the *ART* increases correspondingly. This is because the *OMT* for each multicast member in each M^2R in *PQRS* and the route between multicast member node pair in *MM-MBHA* and *MM-MBHA-CPM* become much complex.

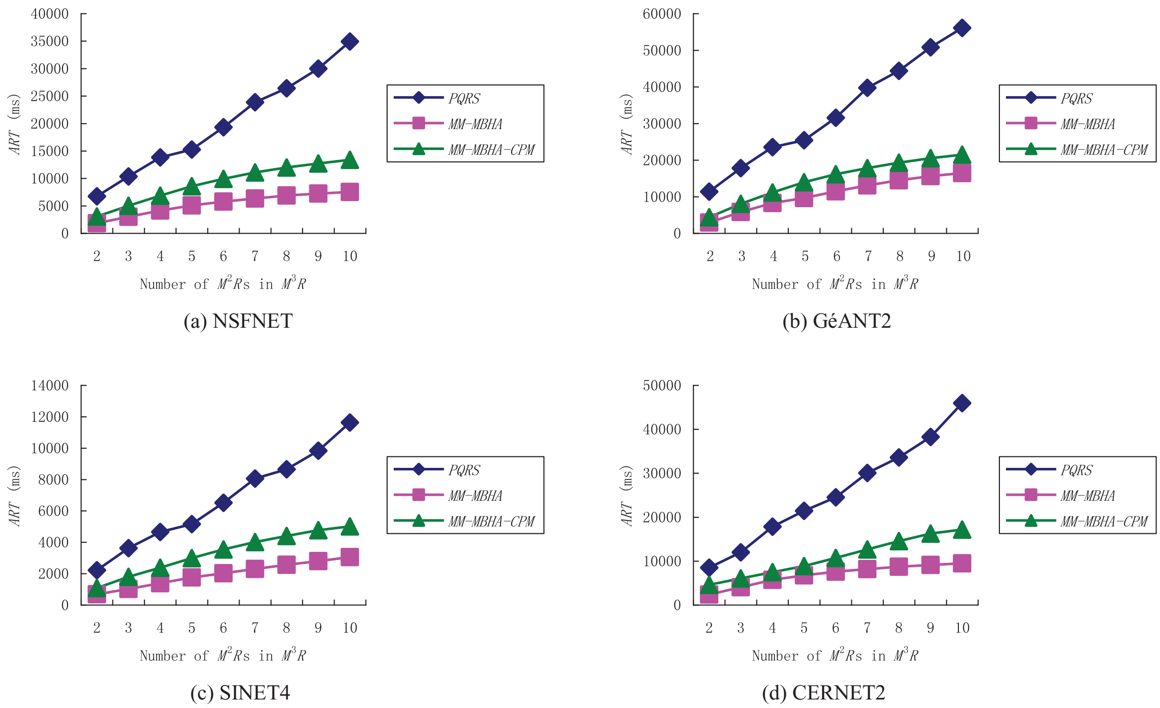

Fig. 9. Comparison of *ART* among *PQRS*, *MM-MBHA* and *MM-MBHA-CPM*.

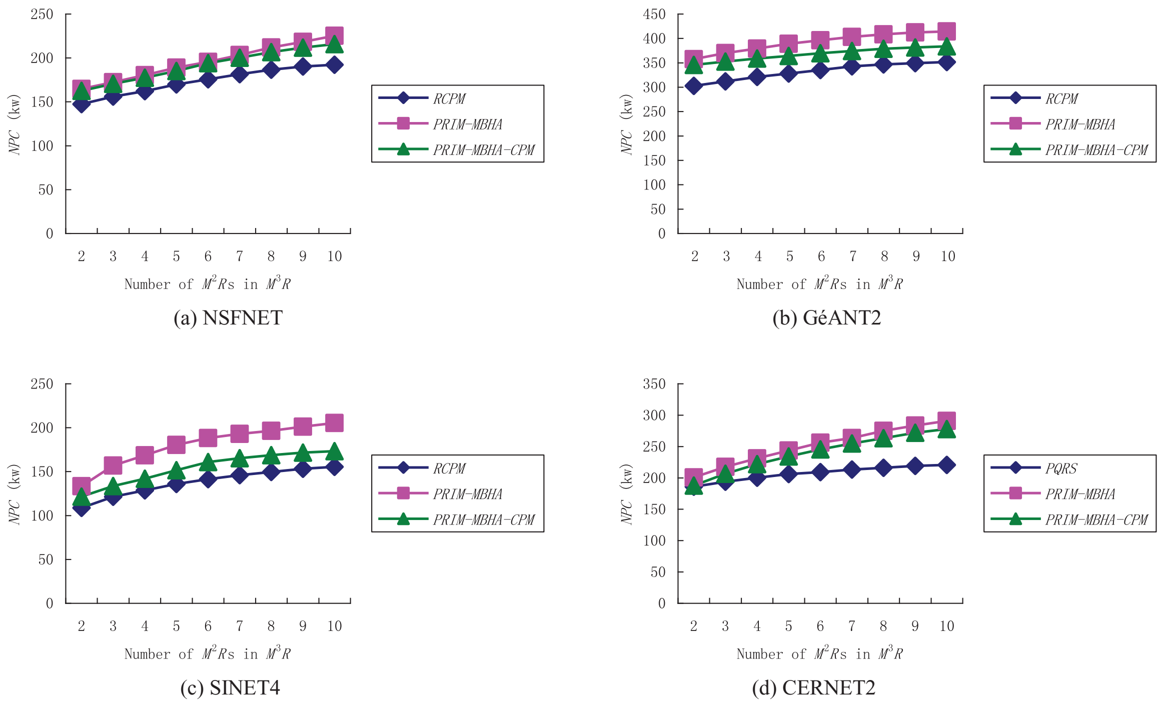

Fig. 10. Comparison of *NPC* among *PQRS*, *PRIM-MBHA* and *PRIM-MBHA-CPM*.

5.3. Comparison with MM-MBHA

To evaluate our proposed scheme further, we also compare it with *PRIM*, which is a classical multicast tree algorithm with time complexity $O(N^4)$. Moreover, we integrate it with *MBHA* (*PRIM-MBHA*), that is, we apply the key idea of *MBHA* when constructing a multicast tree with *PRIM* algorithm. In particular, we take the available capacity of the link between two nodes as the weight, then we apply *PRIM* algorithm to build a minimum spanning tree as the solution

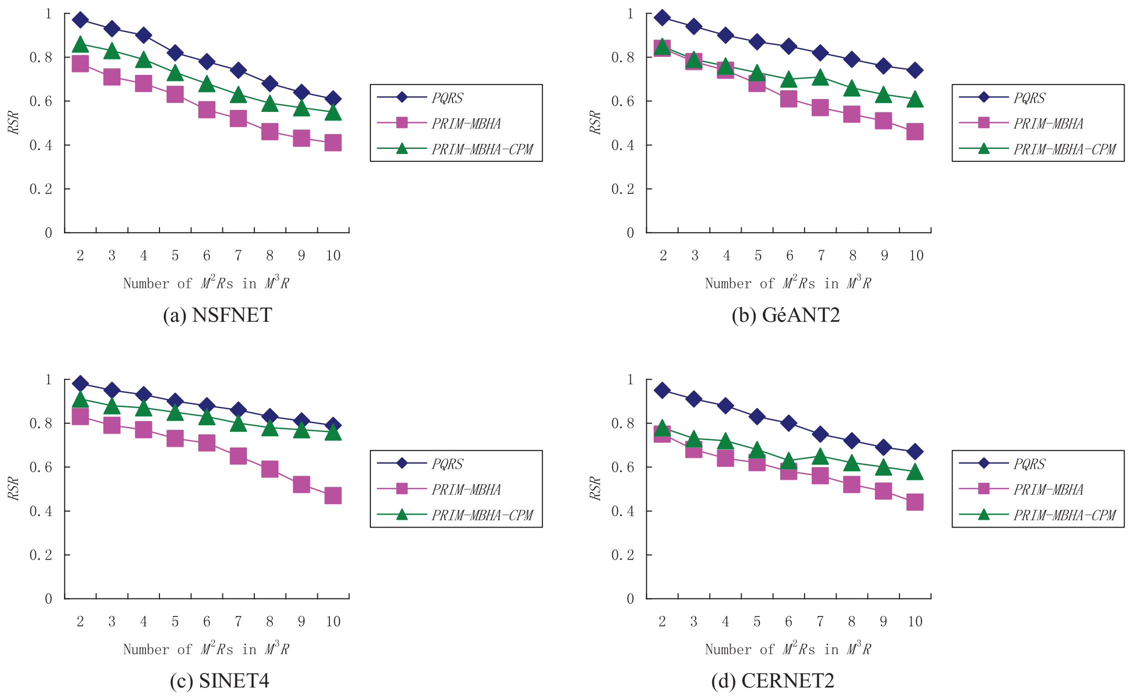

Fig. 11. Comparison of *RSR* among *PQRS*, *PRIM-MBHA* and *PRIM-MBHA-CPM*.

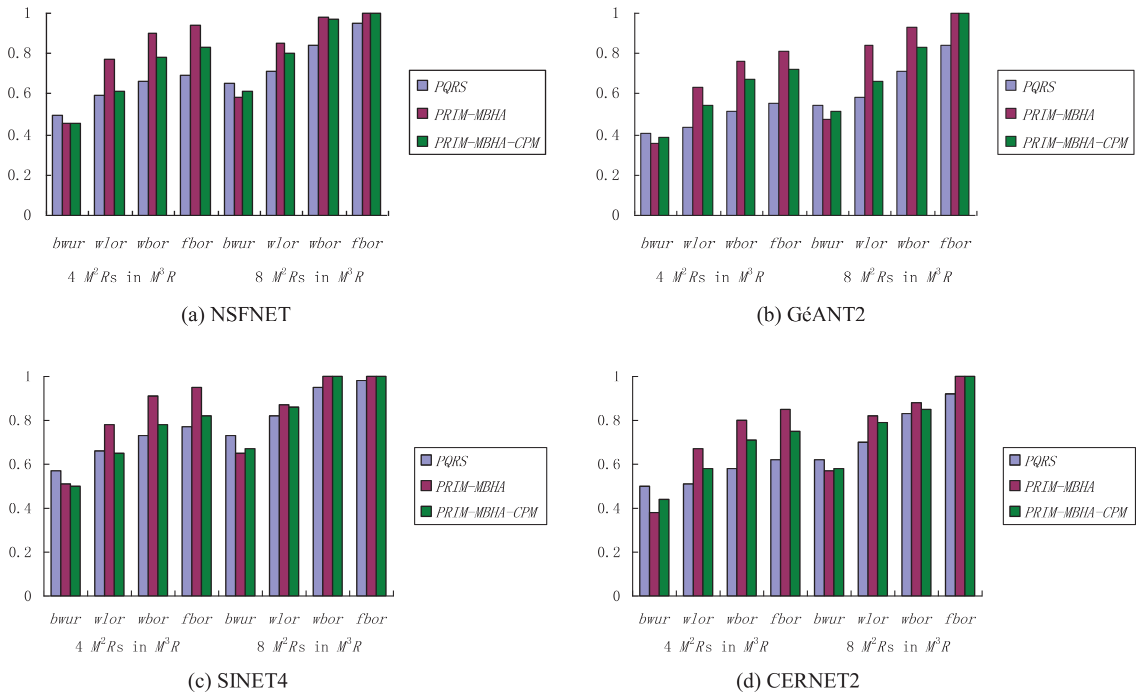

Fig. 12. Comparison of *RUR* among *PQRS*, *PRIM-MBHA* and *PRIM-MBHA-CPM*.

of one-to-many multicast request by choosing links with the least capacity iteratively, afterwards we construct the M^2T by merging all its corresponding minimum spanning trees, finally we get the M^3T by simply merging all M^2Ts. In order to verify the effectiveness of *CPM*, we also integrate it with *PRIM-MBHA* and get the so-called *PRIM-MBHA-CPM*.

Fig. 10 shows the *NPC* of *PQRS*, *PRIM-MBHA* and *PRIM-MBHA-CPM* over the four topologies. We can observe that *PRIM-MBHA* consumes the most power, because it considers

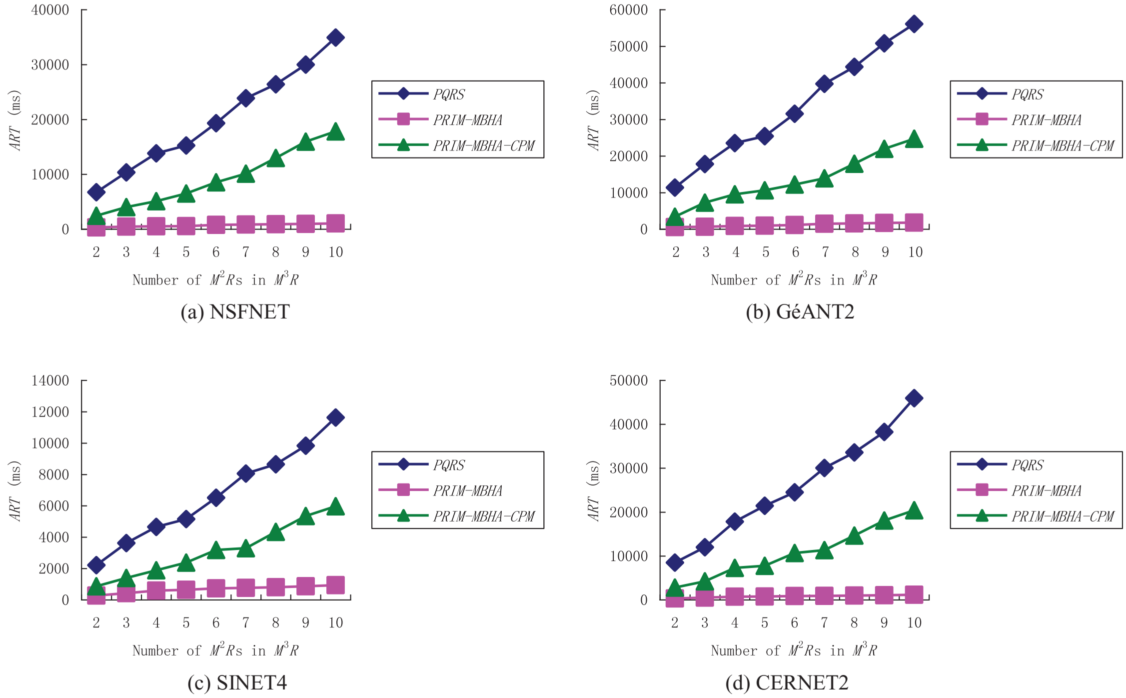

Fig. 13. Comparison of *ART* among *PQRS*, *PRIM-MBHA* and *PRIM-MBHA-CPM*.

power saving only from the viewpoint of the smallest amount of hops along the route. As *CPM* can help choose the link more power-efficiently with various factors considered when routing, the power consumption of *PRIM-MBHA-CPM* is less than that of *PRIM-MBHA*. However, *PRIM-MBHA-CPM* still consumes more power than *PQRS* for not having the multiplexing phase of *PQRS* and thus having more resources occupied and more components kept active.

Fig. 11 shows that the *RSR* of *PQRS* is higher than that of *PRIM-MBHA-CPM* over the four topologies. This is because the multiplexing phase of *PQRS* improves the *RSR*. Meanwhile, the *RSR* of *PRIM-MBHA-CPM* is higher than that of *PRIM-MBHA*, the reason is that *CPM* considers QoS evaluation and then can improve the *RSR* to some extent.

Fig. 12 shows that *bwu*, *wlo*, *wbo* and *fbo* of *PQRS* are better than those of *PRIM-MBHA* and *PRIM-MBHA-CPM* over the four topologies. This is because the multiplexing phase of *PQRS* uses the already-in-use components as many as possible and thus improves *RUR* further. In addition, *bwu*, *wlo*, *wbo* and *fbo* of *PRIM-MBHA-CPM* are better than that of *PRIM-MBHA* for the contribution of *CPM*.

In Fig. 13, we compare the *ART* of *PQRS*, *PRIM-MBHA*, and *PRIM-MBHA-CPM* over the four topologies. Similar to Fig. 9, the *ART* of *PQRS* is longer than that of *PRIM-MBHA* and *PRIM-MBHA-CPM*. The calculation of *CP* for each link and generation of *OMTs* for each multicast member in each M^2R in *PQRS* and *PRIM-MBHA-CPM* brings the main overheads. In addition, the multiplexing phase in *PQRS* makes it consume more time than *PRIM-MBHA-CPM*.

The reasons why we get such performance comparison results among *PQRS*, *PRIM-MBHA*, and *PRIM-MBHA-CPM* are similar to those explained in Section 5.2.

In summary, *PQRS* is more power-efficient with stronger QoS support and better resource utilization than others at the cost of longer running time.

6. Conclusion

In this paper, a power-efficient QoS routing scheme is proposed for multiple many-to-many multicast requests with given static traffic demands in green multi-granularity transport networks. It not only deals with their diversified QoS requirements, but also finds routes for them with power consumption, QoS evaluation and resource utilization evaluation optimized. In particular, a probability model is established to facilitate the most eligible links to be chosen when routing. A heuristic algorithm is proposed to complete routing for applications effectively and efficiently. Simulation results demonstrate that our proposed scheme is superior to certain existing routing schemes in terms of the comprehensive performance.

There are a lot of works to be done in the future. On one hand, we will improve our devised *CPM* further to exploit more effective way of probability modeling and computation, so that more appropriate links can be chosen when routing at the same time the runtime overhead can be reduced significantly. On the other hand, we will try to use some distributed swarm intelligence algorithms, such as ant colony [52] or beehive colony algorithms [53], to build the multicast tree with performance optimized. In addition, we plan to implement our proposed scheme in a prototype system to test it in CERNET2 to make it more practical.

Acknowledgments

This work is supported by the National Science Foundation for Distinguished Young Scholars of China under Grant No. 61225012 and No. 71325002; the National Natural Science Foundation of China under Grant No. 61572123; the Specialized Research Fund of the Doctoral Program of Higher Education for the Priority Development Areas under Grant No. 20120042130003.

The authors would like to thank the anonymous reviewers for their comments to improve the paper.

References

[1] S. Zeadally, S.U. Khan, N. Chilamkurti, Energy-efficient networking: past, present, and future, J.Supercomput 62 (3) (2012) 1093–1118.
[2] M. Gupta, S. Singh, Greening of the Internet, in: Proceedings of the ACM SIGCOMM, 2003.
[3] C. Lin, Y. Tian, M. Yao, Green network and green evaluation: mechanism, modeling and evaluation, Chin. J. Comput. 34 (4) (2011) 593–612 in Chinese with English Abstract.
[4] W. Fu, T. Song, A frequency adjustment architecture for energy efficient router, in: Proceedings of the ACM SIGCOMM, 2012.
[5] S. Nedevschi, L. Popa, G. Iannaccone, S. Ratnasamy, D. Wetherall, Reducing network energy consumption via sleeping and rate-adaptation, in: Proceedings of the USENIX NSDI, 2008.
[6] M. Xia, M. Tornatore, Y. Zhang, P. Chowdhury, C. Martel, B. Mukherjee, Greening the optical backbone network: a traffic engineering approach, in: Proceedings of the IEEE ICC, 2010.
[7] X. Cao, V. Anand, C. Qiao, Framework for waveband switching in multigranular optical networks : part II – wavelength/waveband conversion and survivability, J. Opt. Netw 6 (1) (2007) 48–62.
[8] Y. Cao, Z. Sun, Routing in delay/disruption tolerant networks: a taxonomy, survey and challenges, IEEE Commun. Surv. Tutor 15 (2) (2013) 654–677.
[9] S. Ehsan, B. Hamdaoui, A survey on energy-efficient routing techniques with QoS assurances for wireless multimedia sensor networks, IEEE Commun. Surv. Tutor 14 (2) (2012) 265–278.
[10] N.A. Pantazis, S.A. Nikolidakis, D.D. Vergados, Energy-efficient routing protocols in wireless sensor networks: a survey, IEEE Commun. Surv. Tutor 15 (2) (2013) 551–591.
[11] Y.M. Kim, E.J. Lee, H.S. Park, J.K. Choi, H.S. Park, Ant colony based self-adaptive energy saving routing for energy efficient Internet, Comput. Netw 56 (10) (2012) 2343–2354.
[12] A. Cianfrani, V. Eramo, M. Listanti, M. Marazza, E. Vittorini, An energy saving routing algorithm for a green OSPF protocol, in: Proceedings of the IEEE INFOCOM, 2010.
[13] Y. Yang, D. Wang, M. Xu, S. Li, Hop-by-hop computing for green Internet routing, in: Proceedings of the IEEE ICNP, 2013.
[14] Y. Fazili, A. Nafarieh, W. Robertson, Hybrid energy-aware and SLA-based routing mechanism over optical networks, Procedia Computer Science 19 (2013) 1151–1158.
[15] E. Yetqiner, G.N. Rouskas, Power efficient traffic grooming in optical WDM networks, in: Proceedings of the IEEE GLOBECOM, 2009.
[16] M.M. Hasan, F. Farahmand, A.N. Patel, J.P. Jue, Traffic grooming in green optical networks, in: Proceedings of the IEEE ICC, 2010.
[17] A. Ebrahimzadeh, A.G. Rahbar, B. Alizadeh, QoS aware green routing and wavelength assignment in core WDM networks, J. Netw. Comput. Appl 53 (2015) 1–13.
[18] R. Schatz, M. Fiedler, L. Skorin-Kapov, QoE-based network and application management, in: S. Moller, A. Raake (Eds.), Quality of Experience, Springer, New York, 2014, pp. 411–426.
[19] F. Idzikowski, E. Bonetto, L. Chiaraviglio, R. Duque, F. Jiménez, E.L. Rouzic, F. Musumeci, W.V. Heddeghem, J.L. Vizcaino, Y. Ye, Trend in energy-aware adaptive routing solutions, IEEE Commun. Mag 51 (11) (2013) 94–104.
[20] C. Panarello, A. Lombardo, G. Schembra, L. Chiaraviglio, M. Mellia, Energy saving and network performance: a trade-off approach, in: Proceedings of the e-Energy, 2010.
[21] A. Sánchez-Squella, R. Ortega, R. Griño, S. Malo, Dynamic energy router, IEEE Control Syst 30 (6) (2010) 72–80.
[22] C. Hu, C. Wu, W. Xiong, B. Wang, J. Wu, M. Jiang, On the design of green reconfigurable router toward energy efficient Internet, IEEE Commun. Mag 49 (6) (2011) 83–87.
[23] B. Wu, S. Fu, X. Jiang, H. Wen, Joint scheduling and routing for QoS guaranteed packet transmission in energy efficient reconfigurable WDM mesh networks, IEEE J. Sel. Areas Commun 32 (8) (2014) 1533–1541.
[24] Y. Wu, B. Guo, Y. Shen, J. Wang, X. Liu, A cross-layer optimization and design approach under QoS constraints for green IP over WDM networks, Comput. Netw 76 (2015) 177–190.
[25] S.K. Dey, A. Adhya, IP-over-WDM network design methodology to improve efficiency in overall expenditure due to cost and energy consumption, J. Opt. Commun. Netw 7 (6) (2015) 563–577.
[26] G. Wu, G. Mohan, Power-efficient integrated routing of sublambda connection requests with traffic splitting in IP over WDM networks, Comput. Netw 70 (2014) 16–29.
[27] A. Coiro, M. Listanti, A. Valenti, Impact of energy-aware topology design and adaptive routing at different layers in IP over WDM networks, in: Proceedings of the NETWORKS, 2012.
[28] N. Charbonneau, V.M. Vokkarane, A survey of advance reservation routing and wavelength assignment in wavelength–routed wdm networks, IEEE Commun. Surv. Tutor 14 (4) (2012) 1037–1064.
[29] X. Wang, H. Cheng, K. Li, J. Li, J. Sun, A cross-layer optimization based integrated routing and grooming algorithm for green multi-granularity transport networks, J Parallel Distrib. Comput 73 (6) (2013) 807–822.
[30] S. Avallone, G. Ventre, Energy efficient online routing of flows with additive constraints, Comput. Netw 56 (10) (2012) 2368–2382.
[31] G. Fang, GRASP-BSMA: a fast algorithm for delay constrained multicast routing, in: Proceedings of the IEEE ICC, 2012.
[32] M.T. Chen, B.M.T. Lin, S.S. Tseng, Multicast routing and wavelength assignment with delay constraints in WDM networks with heterogeneous capabilities, J. Netw. Comput. Appl 31 (1) (2008) 47–65.
[33] R. Lin, W.D. Zhong, S.K. Bose, M. Zukerman, Constrained light-tree design for WDM mesh networks with multicast traffic grooming, Opt. Switch. Network 10 (2013) 233–245.
[34] N. Sambo, G. Meloni, G. Berrettini, F. Paolucci, A. Malacarne, A. Bogoni, F. Cugini, L. Potì, P. Castoldi, Demonstration of data and control plane for optical multicast at 100 and 200 Gb/s with and without frequency conversion, J. Opt. Commun. Netw 5 (7) (2013) 667–676.
[35] R. Maniyar, P. Ghosh, A. Sen, A unified approach for multiple multicast tree construction and max-min fair rate allocation, in: Proceedings of the IEEE HPSR, 2009.
[36] L.S. Randaccio, L. Atzori, Group multicast routing problem: a genetic algorithms based approach, Comput. Netw 51 (14) (2007) 3989–4004.
[37] W.S. Hu, Q.J. Zeng, Multicasting optical cross connects employing splitter-and-delivery switch, IEEE Photonics Technol. Lett 10 (7) (1998) 970–972.
[38] A Maher, J.S. Deogun, Power-efficient design of multicast wavelength-routed networks, IEEE J. Sel. Areas Commun 18 (10) (2000) 1852–1862.
[39] S. Blake, D. Black, M. Carlson, E. Davies, Z. Wang, W. Weiss, An architecture for differentiated services, Internet RFC 2475 (1998).
[40] End-user multimedia QoS categories ITU-T G.1010, 2001.
[41] J.M. Blanquer, A. Batchelli, K. Schauser, R. Wolski, Quorum, flexible quality of service for Internet services, in: Proceedings of the USDI, 2005.
[42] A. Orda, A. Sprintson, Precomputation schemes for QoS routing, IEEE/ACM Trans. Netw 11 (4) (2003) 578–591.
[43] M. Li, Y.L. Wu, C.R. Chang, Available bandwidth estimation for the network paths with multiple tight links and bursty traffic, J. Netw. Comput. Appl. 36 (2013) 353–367.
[44] J. Li, L. Zhang, Y. Shi, Research on evaluation model of organizational knowledge assets, J. Inf. Knowl.. Manag. 7 (1) (2008) 1–8.
[45] W. Pedrycz, E. Ekel, R. Parreiras, Fuzzy Multi-Criteria Decision-Making Models, Methods and Applications, Wiley Press, 2011.
[46] B. Mukherjee, Optical WDM Networks, Springer, New York, 2006.
[47] X. Jia, N. Pissinou, K. Makki, A real-time multicast routing algorithm for multimedia applications, Computer, Communications 20 (12) (1997) 1098–1106.
[48] G. Shen, R.S. Tucker, Energy-minimized design for IP over WDM networks, IEEE/OSA J. Opt. Commun. Networking 1 (1) (2009) 176–186.
[49] Cisco CRS-3 [Online] Available: http://www.cisco.com/web/solutions/sp/ip_ngn/index.html
[50] Cisco ONS 15454 [Online] Available: http://www.cisco.com/en/US/products/hw/optical/ps2006/index.html
[51] D.S. Malik, Data Structures Using C++, second ed., Course Technology, Boston, 2009.
[52] T. Stützle, M. López-Ibáñez, M. Dorigo, A concise overview of applications of ant colony optimization, in: J.J. Cochran (Ed.), Wiley Encyclopedia of Operations Research and Management Science, John Wiley & Sons, 2011, pp. 896–911.
[53] D. Karaboga, B. Akay, A comparative study of artificial bee colony algorithm, Appl. Math. Comput 214 (1) (2009) 108–132.

Xingwei Wang received the B.S., M.S., and Ph.D.degrees in computer science from the Northeastern University, Shenyang, China, in 1989, 1992, and 1998 respectively. He is currently a Professor at the College of Software, Northeastern University. He has published over 100 research papers. His research interests include cloud computing and future Internet, etc.

Dapeng Qu received the B.S. degree in applied mathematics and computer science from Central South University, Changsha, China, in 2003, and 2006 respectively, and Ph.D. degree in computer science from the Northeastern University, Shenyang, China, in 2012. He is currently an associate professor at the College of Information, Liaoning University. His research interests include computer networking and future Internet, etc.

Min Huang received the B.S. degree in automatic instrument, the M.S. degree in systems engineering, and Ph.D. degree in control theory from the Northeastern University, Shenyang, China, in 1990, 1993, and 1999 respectively. She is currently a Professor at the College of Information Science and Engineering, Northeastern University. She has published over 100 research papers. Her research interests include the modeling and optimization for the logistics and supply chain system, etc.

Keqin Li received the B.S. degree in computer science from Tsinghua University, Beijing, China, in 1985, and Ph.D. degree in computer science from the University of Houston, Texas, USA, in 1990. He is currently a SUNY distinguished professor of computer science in State University of New York at New Paltz. He has published over 200 journal articles, book chapters, and research papers in refereed international conference proceedings. His research interests include parallel and distributed computing and computer networking, etc.

Sajal K Das received the BS degree in computer science from Calcutta University, Kolkata, India, in 1983, the MS degree in computer science from the Indian Institute of Science, Bangaluru, India, in 1984, and the PhD degree in computer science from the University of Central Florida, Orlando, in 1988. He is currently with the Department of Computer Science, Missouri University of Science and Technology. He is the author of more than 400 published papers and more than 35 invited book chapters. He is a Fellow of the IEEE.

Jinhong Zhang received the B.S. degree in automation from Hangzhou Dianzi University, Hangzhou, China, in 2006, and the M.S. degree in computer science from the Northeastern University, Shenyang, China, in 2011. He is currently a Ph.D. candidate at the College of Information Science and Engineering, Northeastern University. His research interests include green Internet, and energy saving routing schemes, etc.

Ruiyun Yu received the BS degree in mechanical engineering from the Northeastern University, China, in 1997, and the MS and PhD degrees in computer science from the Northeastern University, China, in 2004 and 2009, respectively. He is currently an associate professor in the Software College of Northeastern University, China. His research interests include participatory sensing systems, mobile and pervasive computing, big data analytics, etc.